Use Authorization

In presenting this dissertation in partial fulfillment of the requirements for an advanced degree at Idaho State University, I agree that the Library shall make it freely available for inspection. I further state that permission to download and/or print my dissertation for scholarly purposes may be granted by the Dean of the Graduate School, Dean of my academic division, or by the University Librarian. It is understood that any copying or publication of this dissertation for financial gain shall not be allowed without my written permission.

Signature _____

Nada Abdullah Alomairy

Date _____

APPLICATION OF THE ICRP 67 AND NCRP 156 BIOKINETIC MODELS TO AMERICIUM- 241 WOUND DATA FROM NONHUMAN PRIMATES

By

Nada A. Alomairy

A dissertation

submitted in partial fulfillment

of the requirements for the degree of

Doctor of Philosophy in Nuclear Science and Engineering

Idaho State University

December 2017

To the Graduate Faculty:

The members of the committee appointed to examine the dissertation of **Nada Alomairy** find it satisfactory and recommended that it be accepted.

Dr. Richard Brey
Major Advisor

Dr. Thomas F. Gesell
Committee Member

Dr. Raymond A. Guilmette
Committee Member

Dr. George Imel
Committee Member

Dr. DeWayne Derryberry
Graduate Faculty Representative

AKNOWLEDGEMENTS

I would like to thank my major advisor, Dr. Richard Brey for his excellent guidance and advice. I would like to thank my committee members Dr. Thomas Gesell, Dr. George Imel, and Dr. Raymond Guilmette for valuable comments on my dissertation and for their time and attention. Also, I would like to thank Dr. DeWayne Derryberry for serving as a Graduate Faculty Representative on my committee and for his valuable comments on my hypothesis. I am also thankful for the support I received along the way from my parents and siblings. I would also like to express my thanks to the Saudi Arabia Ministry of Higher Education for their financial support through my doctorate study.

TABLE OF CONTENTS

LIST OF FIGURES

LIST OF TABLES

LIST OF ABBREVIATIONS AND ACRONYMS

Am	Americium
Bq	Becquerel
CIS	Colloidal and Intermediate States
CM	Cortical marrow
CS	Cortical surface
CV	Cortical volume
GI	Gastrointestinal
ICRP	International Commission on Radiological Protection
IDEAS	General Guidelines for the Estimation of Committed Dose from Incorporation Monitoring Data
im	Intramuscular(ly)
IMBA	Integrated Modules for Bioassay Analysis
IMBA UA	Integrated Modules for Bioassay Analysis Uncertainty Analysis
Iv	Intravenous(ly)
LBNL	Lawrence Berkeley National Laboratory
NaI(TI)	Thallium Activated Sodium Iodide Detector
NCRP	National Council on Radiation Protection and Measurements
NHPs	Nonhuman Primates
PABS	Particles, Aggregates and Bound States
Pu	Plutonium
U	Uranium

SF	Scattering Factor
TM	Trabecular marrow
TPA	Trapped Particles and Aggregates
TS	Trabecular surface
TV	Trabecular volume
UA	Uncertainty Analyzer
UBC	Urinary bladder contents
ULI	Upper large intestine
USNRC	United States Nuclear Regulatory Commission

ABSTRACT

Distribution, retention, and excretion of intramuscularly injected ^{241}Am citrate have been investigated in cynomolgus and rhesus nonhuman primates (NHP). Bioassay and retention data, obtained from experiments done by Patricia Durbin and her colleagues at Lawrence Berkeley National Laboratory, were evaluated against the International Commission on Radiological Protection (ICRP 67) ^{241}Am systemic model coupled with to the National Council on Radiation Protection and Measurement wound model (NCRP 156). The default transfer rates suggested in these models were used with the urine and feces excretion data to predict the intake as well as liver and skeleton tissue contents at the time of death. The default models produced adequate fits using urine bioassay data, but the injected activities were over-predicted by as much as 4.41 times and under-predicted by as much as 0.99 times. Poor prediction has been observed in all cases using fecal excretion. The retained activity in the liver and skeleton at the time of death were investigated using the same approach. It appears that the models accurately predict the amount of the activity retention in the skeleton more accurately than in the liver. A practical decision was established whereby the ICRP 67 and NCRP 156 parameters predicted the skeleton retention within 20% of the measured values. The fraction of predicted to measured activity at the time of death in the skeleton was over 1.0 in most cases and accurate predictions were obtained in 7 cases. The predicted activity in skeleton for these cases ranged from 14% under the known value to 17% over. NHPs' urine data and organ retention were compared with data from previously modeled baboons and beagle dogs. About six percent of the injected activity in NHP was excreted in urine and approximately 0.1% in feces in the first 24h. The results from NHP is different from excreta analysis in baboons and beagle dogs. Urinary excretion in the cynomolgus, rhesus, and baboon

NHPs is the dominate pathway of Am-214 clearance, however, the fecal excretion are considered dominate by the end of second week in baboons and the end of the third week in NHPs. Urinary excretion is considered the dominate pathway of clearance in beagle dogs until the end of the experiment. The comparison between NHP and human is difficult due to the differences in the amount of activity translocated or deposited in the liver tissue and non-liver tissues (primarily skeleton), in addition; to the physiological differences between the NHP and human. Another objective of this study was to develop new transfer rate parameters for wound and systemic models in an effort to improve the biokinetic predictions. Estimates of new transfer rates appropriate for the nonhuman primate data were determined by employing a companion program called IMBA-UA. During validation of the suggested transfer rates, it was observed that the optimized parameters predicted the intake in 66% of the tested animals used in this investigation. The activity retained in the skeleton improved in almost all cases where the differences between the predicted and measured activity in a value less than 20%. However, the modified parameters did not improve the fit in three cases where the ratio of observed to predicted values of the χ^2 were less than 0.05. (Work performed with partial support from funding from the National Institute of Allergy and Infectious Diseases under contract HHSN272201000046C).

Chapter 1:

Introduction

1.1. Statement of the Problem

Different radionuclides may be present in the human body as a result of dietary and respiratory intake. Radioactive contaminants can enter the body by essentially five pathways: inhalation, ingestion, injection, absorption from wounds, and absorption through intact skin. Workers have been accidentally exposed to transuranic materials such as Americium. The largest exposure to americium was recorded in 1976 where an ion-exchange column containing about 100 g of ^{241}Am exploded. As a result of this accident, a chemical operator was injured receiving acid burns and superficial cuts on the upper part of his body and from 1 to 5 Ci of ^{241}Am is estimated to have been deposited on the injured worker and on his clothing (McMurray, 1983). The probability of these accidents could increases if there is increased uses of such transuranic materials. Accurately predicting the distribution and retention of radionuclides in humans following intakes is necessary for calculating organ-level absorbed doses and risks.

The International Commission on Radiological Protection (ICRP) Issued Publication 54: Individual Monitoring for Intakes of Radionuclides by Workers: Design and Interpretation (ICRP1988b), which was published in 1988. This ICRP Publication offered recommendations on the "design of individual monitoring programs including the interpretation of results of measurements of intakes of radionuclides by workers" (ICRP78 1997).

ICRP Publication 78 gives general guidance on the "design of individual monitoring programs and the interpretation of measurement results for some radionuclides selected because of their potential importance in occupational exposure". It follows the commission's general

principles of monitoring for the radiation protection of workers. In addition, ICRP 78 provide predictive fractional parameters of anticipated measured quantities of radioactivity associated with exposed individuals, such as body content, organ content, daily urinary excretion, and daily fecal excretion; for different times after a single intake and for routine monitoring. Various organizations such as, ICRP and the National Council on Radiation Protection and Measurement (NCRP) advocate that if there is a potentially significant exposure resulting in an intake of radioactive material by workers, then monitoring programs must be developed which carefully consider the nature, behavior, and both physical and chemical properties of the radioactive materials to be handled (ICRP 78, 1997).

Investigation, modification, and improvement of models describing metabolism and translocation of radioactive materials is difficult using human accident cases. These cases are inappropriate to accurately understand the distribution and retention of ^{241}Am following intake because victims may have been treated either with chelation or excision shortly after exposure (Guilmette et al. 2007). Therefore, experimental animal studies have been widely used to understand the behavior of radioactive materials within living organisms. Unlike human case studies, the intakes in animal experiments are well quantified and controlled. This is never the case when considering accident cases, where the intake can only be inferred based on the use of measurement data and mathematical modeling; in any case, there will be significant uncertainty in intake estimation. Moreover, exposure levels for the multiple experimental animals can be higher than would be appropriate even with human volunteers. Therefore, animal experiments are necessary and useful to develop the kinds of data needed to build models for dose and risk assessments in humans. Most of the animal studies have included intravenously or intramuscularly injected radioactive contaminants to groups of animal species like monkeys,

baboons, and beagle dogs (monkeys by Durbin et al. 1990; beagle dogs by Lloyd et al. 1970; and baboons by Guilmette et al. 1980).

Nonhuman primates (NHP) are phylogenetically and metabolically the closest animals to humans. These experimental animal data have played a big role in constructing and parameterizing the biokinetic models needed for human internal dosimetry including those for Americium. Because of the lack of human data, it is necessary to analyze the experimental animal data available using human biokinetic data available to bench mark the validity of models.

Current compartmental models were used to study the distribution and retention of radioactive materials within primates. One of the most common biokinetic models for americium is the age-dependent model published in ICRP published 67 (ICRP 1993). Data obtained after the intravenous injection of radioactive materials into nonhuman primate can be used to parameterize a systemic model such as the ICRP 67 biokinetic model. ICRP 67 assumes direct and instantaneous injection of ^{241}Am into the bloodstream pathways. However, not all exposures are well reproduced by this scenario. Frequently exposure to radionuclides such as ^{241}Am arise because of contaminated wounds. A model for describing activity entering through wounds was developed by the National Council on Radiation Protection and Measurements (NCRP) published report 156 (NCRP 2006). The kinetics of radioactive materials entering the body via wounds depend on the depth of wound, chemistry of radionuclides, etc, therefore the absorption into the bloodstream might be substantially delayed. The translocation of radioactive materials among compartments is associated with specific transfer rates. The translocation usually is assumed to follow first order kinetics and in some instances involves recycling. These approaches are described in ICRP 67 and NCRP report 156.

Between 1960 and 1985, Patricia Durbin and colleagues performed studies on the distribution of intravenously and intramuscularly injected ^{241}Am in nonhuman primates (NHP) with dosages ranging from 16 to 32 kBq/kg (Table 1.1). The study was conducted at the Lawrence Berkeley Laboratory from1959 through 1982. The advantage of using animals in the biokinetics studies is that animals can be injected with known quantities of radioactive materials in a controlled experiment. As part of the experimental design, serial blood samples were taken and urine and feces samples were collected separately for the duration of the study. The measurements of urine, fecal excretion, blood samples, and organ burden data obtained from twenty animals were used to evaluate the transfer rates among organs using the ICRP67 biokinetic model and NCRP 156 wound model for Am-241.

1.2.The Purpose of the Study

The purpose of the present work was to explain the retention and behavior of ^{241}Am in the human body after shallow, sub-cutis skin-wound-contamination using urinary, fecal, and autopsy data obtained from cynomolgus and rhesus NHPs. This effort was therefore used to evaluate the applicability of ICRP 67 transfer rates coupled with the NCRP 156 transfer rates recommended for humans. The NHPs data were further used to compare and validate the model results obtained from other animal experiments such as those using baboons and beagle dogs.

Twenty cases were administered Am-241 citrate by intermuscular injection (Table 1.1). The ICRP 67 systemic and NCRP 156 wound models were investigated with these data. The measurements of the Am-241 concentration in urine and feces samples obtained from animals post injection but prior to death and their autopsy data were used to evaluate the ICRP 67 biokinetic and NCRP 156 wound models. The combination of the biokientic and wound models were used

to study data from the intramuscularly treated primates, evaluate the default parameters recommended for human, and also to parameterize models for nonhuman primates.

The NCRP default wound model parameters for "strongly" retained radionuclides and ICRP 67 systemic model parameters (Tables 4&5) were used to predict the excretion of Am-241 and the activity found in various organs at the time of death using the known intake for each monkey as reported by Durbin el al. These values were compared to actual experimentally measured nonhuman primate values. The estimated activity of intake, calculated using the default parameters, was compared to the true injected value. The predicted concentration of Am-241 in liver and skeleton at the time of death was compared to the actual measured values obtained postmortem. These data were further used in interspecies comparisons of model efficacy that considered baboon and beagle dog data.

The applicability of transfer rates recommended in ICRP 67 and NCRP 156 for humans to NHP or using NHP data to develop transfer rates potentially applicable to humans is a non-trivial exercise. Therefore; a secondary goal of this project was to alter default wound and systemic model parameters and developed suggestions for wound and systemic model transfer rate values based on bioassay and autopsy data of NHPs that improved the predictive capability of current models. The effort employed IMBA Professional Plus and the IMBA Uncertainty Analyzer software for determining the most representative distributions of various transfer rate values based upon the primate data. The usefulness of the NHP model to humans is subject to learned interpretation.

Table 1.1. Summary of injection data. Age (d) refer to the elapsed days from injection to sacrifice.

Case[a]	Mode[b]	Days from injection to death (d)	Age at the Time of Death (Y)	Weight (kg)	Injection Amount (Bq)
C155F	im	8	>7.5	3.97	3.70×10^4
C41F	iv	8	2.5	2.5	7.40×10^4
C42F	iv	8	>7.5	3.6	7.40×10^4
C138F	im	8	>5	3.15	7.47×10^4
C55F	im	21	>7.5	NA	7.36×10^4
C6F	im	31	7.6	2.50	7.70×10^4
C44F	im	42	6.7	2.80	7.47×10^4
C56F	im	63	>5.6	3.50	7.33×10^4
C146M	im	64	>6.6	5.33	2.00×10^4
C81F	im	81	>5.3	2.81	7.47×10^4
C162F	im	102	>6.8	2.67	1.18×10^4
R189M	im	110	13.3	4.14	5.81×10^4
C72F	iv	112	4	2.3	7.40×10^4
C157F	im	156	>7.3	3.80	1.96×10^4
C73F	iv	168	6	2.9	7.40×10^4
C158F	im	211	>7.1	3.60	1.96×10^4
R118M	im	223	14.6	9.70	12.1×10^4
C57F	im	224	4.7	3.80	7.33×10^4
C110F	im	226	6.6	3.94	3.66×10^4
C156F	im	301	>7.3	3.80	1.96×10^4
C45F	im	336	8.4	4.10	7.33×10^4
C46F	im	735	>7.5	4.77	7.47×10^4
C54F	im	938	>8	2.86	7.40×10^4
C76F	iv	973	>6	2.5	7.40×10^4
C78F	im	1,037	>14.8	4.17	5.44×10^4
C75F	iv	2,199	>6	3.7	7.40×10^4

[a]M= male, F= female

[b]im= intermuscular, iv= intravenous

1.3. Hypothesis Statements

1.3.1. Predictability of NCRP report No.156 and ICRP 67 models for macaques

The validity of NCRP wound and ICRP 67 models will be evaluate using the following hypothesis:

First Criterion

First Null Hypothesis ($H_{1,0}$):

The default transfer rates of Am-241 employed within the ICRP 67 biokinetic model and the retention equation parameters employed within the NCRP report No.156 may not be used to predict excretion observed post injection of Am-241 citrate in macaques monkeys.

First Alternate Hypothesis ($H_{1,a}$):

The transfer rate of the Am-241 biokinetic model published in ICRP 67 and the retention equation parameters employed within the NCRP report No.156 do predict excretion observed post injection of Am-241 citrate in macaques monkeys.

Decision Rule #1: The null hypothesis will be rejected if it is determined that the chi-square (χ^2) value evaluated using these data is such that ($P< 0.05$). We will consider this evidence that the data fails to provide support by which the null hypothesis may be rejected. As such, the alternate hypothesis will be supported.

Second Criterion

Second Null Hypothesis ($H_{2,0}$):

The default transfer rates of Am-241 employed within the ICRP 67 biokinetic model and the retention equation parameters employed within the NCRP report No.156 may not be used to predict deposition observed post injection of Am-241 citrate in macaques monkeys.

Second Alternate Hypothesis ($H_{2,a}$):

The transfer rate of the Am-241 biokinetic model published in ICRP 67 and the retention equation parameters employed within the NCRP report No.156 do predict deposition observed post injection of Am-241 citrate in macaques monkeys.

Decision Rule #2: The null hypothesis will be rejected if it is determined that the chi-square (χ^2) value evaluated using these data is such that (P< 0.05). We will consider this evidence that the data fails to provide support by which the null hypothesis may be rejected. As such, the alternate hypothesis will be supported.

Third Criterion

Third Null Hypothesis ($H_{3,0}$):

There is significant difference between the estimated activity of intake, which will be calculated using human reference models, and the true injected value.

Third Alternate Hypothesis ($H_{3,a}$):

There is a no significant difference in the estimated activity of intake, which will be calculated using human reference models, and the true injected value.

Decision Rule #3: the null hypothesis will be rejected if it is determined that the difference in the predicted intake activity and the true injected value is more than 20%. Otherwise, the alternate hypothesis will be supported.

Forth Criterion

Forth Null Hypothesis ($H_{4,0}$):

There is significant difference between the estimated activity in the liver and skeleton using human reference models, and the true measured activity at the time of death.

Forth Alternate Hypothesis ($H_{4,a}$):

There is no significant difference between the estimated activity in the liver and skeleton using human reference models, and the true measured activity at the time of death.

Decision Rule #4: the null hypothesis will be rejected if it is determined that the difference in the measured and the predicted activity in the liver and skeleton value is more than 20%. Otherwise, the alternate hypothesis will be support.

1.3.2. Modification of the Transfer Rates

Fifth Criterion

The fourth Hypothesis deals with the potential to alter default wound and systemic model parameters in the effort to improve the biokinetic prediction of Am-241 translocation. This hypothesis is defined as follow:

Fifth Null Hypothesis ($H_{5,0}$):

The NCRP 156 wound retention parameters and the ICRP 67 transfer rates cannot be modified to better predict the excretion, retention, and deposition of Am-241 in macaques.

Fifth Alternate Hypothesis ($H_{5,a}$):

The NCRP 156 wound retention parameters and the ICRP 67 transfer rates can be modified to better predict the excretion, retention, and deposition of Am-241 in macaques.

Decision Rule #5: The modified retention and transfer rates are considered able to improve the model if the optimization of the retention and transfer rates can increase the predictability of the model to within 20% of the default model prediction.

Chapter 2:

Background

2.1. General Concepts Of Internal Dosimetry

Internal doses are calculated indirectly using measured quantities such as excretion rates, environmental monitoring data, and body or organ activity using the appropriate biokinetic and dosimetric models.

To estimate the absorbed dose received by the whole body or by a particular organ or tissue, two basic quantities are needed after the quantity of intake is determined:

1) Number of transformation that have occurred in the source organ due to the activity deposited in the organ that is calculated using the biokinetic model, which describes the translocation of a radionuclides throughout the body.
2) Energy absorbed in the target organ due to the disintegrations occurring in the source organ.

Internal dose assessments may be categorized as either prospective or retrospective. The intake in a prospective dose assessment is known from an understanding of the amount of radioactive materials in the environment. This information is used to calculate the absorbed doses to organs. The intake in retrospective dose assessment is assessed by evaluating the amount of radioactive materials present in the body or excreta after internal contamination took place. Such a retrospective analysis involves a process to evaluate the intake from measurement data and then calculating the dose based on the best estimate of the intake (Etherington et al. 2003).

Different radionuclides are commonly present in the human body as a result of dietary intake and respiratory intake (Table 2.1). Some of these radioactive materials are generated from cosmic ray interaction with the atmosphere. The most common natural radionuclides produced by this mechanism are: ^{3}H, ^{7}Be, ^{14}C. Some of radionuclides arise from the global fallout following

the numerous atomic weapon tests in the atmosphere carried out during the sixties and seventies (Luciani 2002). Yet other radionuclides exist naturally in the earth's crust and are taken into the body by ingestion or inhalation. These either have very long half-lives comparable to the age of the parent or are continuously generated by decay of a long-lived parent.

Table 2.1. Typical values of human body content of main radionuclides found in the environment (Luciani 2002).

Radionuclides	Amount (Bq)	Origin
^{3}H	30	Global fallout and natural
^{14}C	10^{2}-10^{3}	"
^{40}K	4-5.10^{3}	Natural
^{87}Rb	700	"
^{226}Ra	1-10	"
^{228}Ra	0.4	"
^{214}Pd, ^{214}Bi	40	"
$^{235,238}U$	10^{5}	"
^{137}Cs	100	Global fallout
^{90}Sr-^{90}Y	30	"
$^{239,240}Pu$	0.4	"

Radionuclides can enter the body by five pathways: Inhalation, ingestion, injection, and absorption through skin. Figure 1.1 shows the possible paths of intake (Luciani 2002).

Contamination of food or drinking water are examples of problems which could lead to the ingestion of radioactive materials as would be the transfer of the radioactive materials to the mouth following a contamination of the hands. Typically, ingestion can be an important pathway for workers if poor hygienic practices are used. Contamination of a wound or intravenous injection for therapeutic and diagnostic purposes in nuclear medicine could lead to radionuclides being directly transferred to the blood stream. About 2,100 wound contamination events involving radioactive materials have been cited in the literature (NCRP 2006).

The most widely encountered pathway of intake from the environment is through inhalation. The activity of the radionuclide is directly absorbed in the blood in a process similar to gaseous exchange. Although skin is a good barrier against the penetration of radioactive materials into the body, a few materials such as tritiated water and iodine may be absorbed by the skin and translocated to body fluids. Increasing use of radiopharmaceuticals for diagnostic and therapeutic purposes lead to the realization that the injection pathway is becoming one of the most common pathways for radioactive materials to enter the human body (Luciani 2002).

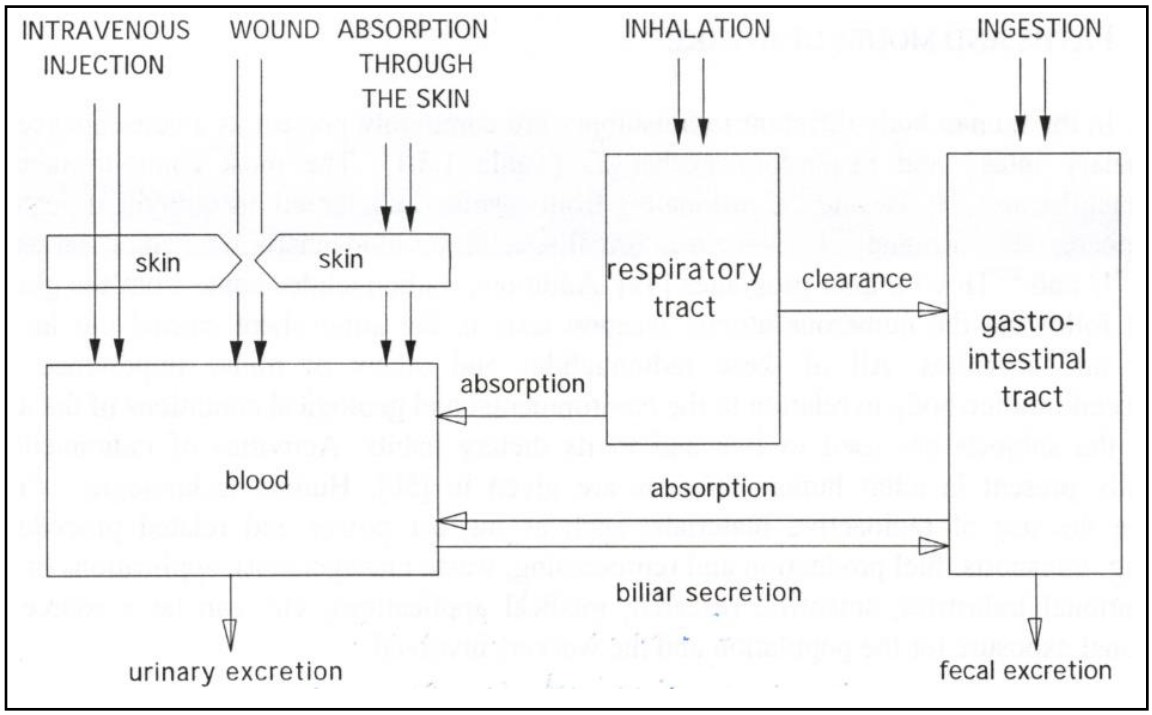

Figure 1.1. The possible paths of intake (Luciani 2002)

The ICRP and NCRP have developed systemic and wound models to describe the behavior of radioactive materials that have entered the human body via one of the five pathways as well as help in assessment of intake and doses from sets of bioassay data.

2.2.Americium

Americium, atomic number 95, is a silvery, ductile, very malleable, non-magnetic metal that is a solid under normal conditions, melts at 1,176 ^{o}c , boils at 2,001 ^{o}c , and has an electron outer shell configuration of $5f_7\ 7S_2$. It is a synthetic radioactive element in the actinide series of elements, which starts with Actinium (Ac, Z= 89) and ends with Lawrencium (Lr, Z= 103). The transuranic elements of the actinide series are located below the lanthanide elements in the periodic table. Americium was first produced in 1944 by Glenn T. Seaborg's group at the University of California, Berkeley, using a 60-inch cyclotron (EPA. 2010). Americium does not have any stable isotopes and does not occur naturally. It is created from plutonium production activities, and is produced by successive neutron capture reactions by plutonium isotopes.

There are sixteen known isotopes of americium and all of them are radioactive. The most common forms of americium are Am-241, Am-242m, Am-242, and Am-243 (Peterson 2007).

Considering the sixteen radioactive isotopes of americium, only three have half-lives long enough to justify a concern according to the Department of Energy (DOE) including: Americium-241, Americium-242m, and Americium-243. The half-lives of these three isotopes range from 150 to 7,400 years, while the half-life of the other isotopes is less than 3 days. These values are reported in Table 2.2.

The most prevalent isotope at DOE sites, such as Hanford, is Americium-241. Americium-241 is considered to be an important component of contamination at several facilities due to the high occurrence of this radioactive element in the cases of accidental internal exposure. Americium-241 ($T_{1/2}$, 433 years; 5.48-MeV alpha particles, 60-keV gamma rays) is a neutron captures product created from U-238 by successive neutron captures to form Plutonium-241 (half-life of 14 years), which decays by isobaric transition (beta emission) to Am-241 (half-life of 433 years). When

plutonium-239 (half-life of 24,100 years) absorbs two neutrons it produces plutonium-241, which later decays by isobaric transition, emitting a negatron to eventually produce americium-241. Americium-241 is a decay product of plutonium and its decays by emitting an alpha particle with attendant gamma radiation. Americium-242m has a half-life of 150 years, and it decays by isomeric transition. Americium-243, which has a 7,400 years' half-life, generally is not a major concern at DOE sites given its low abundance relative to americium-241, and its low specific activity. Americium-243 is produced in a similar fashion by the decay of plutonium-243, and it is also decays by isomeric transition. It alternately is generated by the successive absorption of two neutrons by the Americium-241 isotope. Americium-241 has a high specific activity of 1.3e+11 Bq/g, emitting 7×10^9 alpha particle/ mg/ minute, while Americium-243 has a specific alpha activity 17-times lower than Americium-241 (Peterson 2007).

Americium is commonly used in smoke detectors. The radionuclide used in ionizing smoke detectors is an oxide of Americium-241, which is bonded to a metallic foil and seated in an ionization chamber inside the detector. It is also used with beryllium as a portable source for neutrons, (α,n) reaction; for crystal research; and as a target material in nuclear reactions in particle accelerators to produce even heavier elements (Peterson 2007). Americium-241 can pose significant health effects if it is inadvertently or deliberately absorbed, injected, or ingested within human bodies.

Table 2.2. Radioactive Properties of Key Americium Isotopes and Associated Radionuclide (Peterson 2007).

Isotope	Half-life ($T_{1/2}$)	Specific Activity (Ci/g)	Decay Mode	Alpha (α) MeV	Beta (β)MeV	Gamma (γ)MeV
Am-241	430 yr.	3.5	α	5.5	0.052	0.033
Am-242m	150 yr.	9.8	IT	0.025	0.044	0.0051
Am-242	16 hr.	820,000	B, EC	-	0.18	0.018
Am-243	7,400 yr.	0.2	α	5.3	0.022	0.055
Am-239	11.9 h	-	α	133.3	13.6	-

IT = isomeric transition, EC = electron capture, Ci = curie, g = gram, and MeV = million electron volts (Radiation Energy).

2.3.Biokinetics of Americium

2.3.1. ICRP 67 Systemic Model for Americium

The International Commission on Radiological Protection (ICRP) has developed a series of compartmental systemic biokinetic models. The translocation of radioactive materials among compartments is assumed to follow first order kinetics. A generalized expression for this approach can be written as (Jacquez 1972):

$$\frac{dq(t)}{dt} = (R - \lambda_R I)\, q(t), \qquad q(0) = q_0, \qquad \text{(Equation 1)}$$

Where:

q(t)= the vector of the amount of activity in the nth compartment at time t.

R= the matrix of the transfer rates.

I= the unit matrix.

$\boldsymbol{q_0}$= the matrix of initial conditions.

$\boldsymbol{\lambda_R}$ = the physical decay constant.

ICRP published in ICRP 67 a compartmental model of the kinetics of ingested americium in humans (Figure 2.2) with its associated transfer rates. This specific model is similar to the plutonium model, but this model has been modified and expanded for americium. The model

begins with Americium in the blood as a general transfer compartment. The blood delivers americium to the skeleton, liver, and other tissues. The excretion pathways that are included in this model are liver to feces and plasma to urine. Excretion to urine or feces is highly dependent on the individual's age and the transfer rate coefficients among compartments (Table 2.3) (ICRP67 1993).

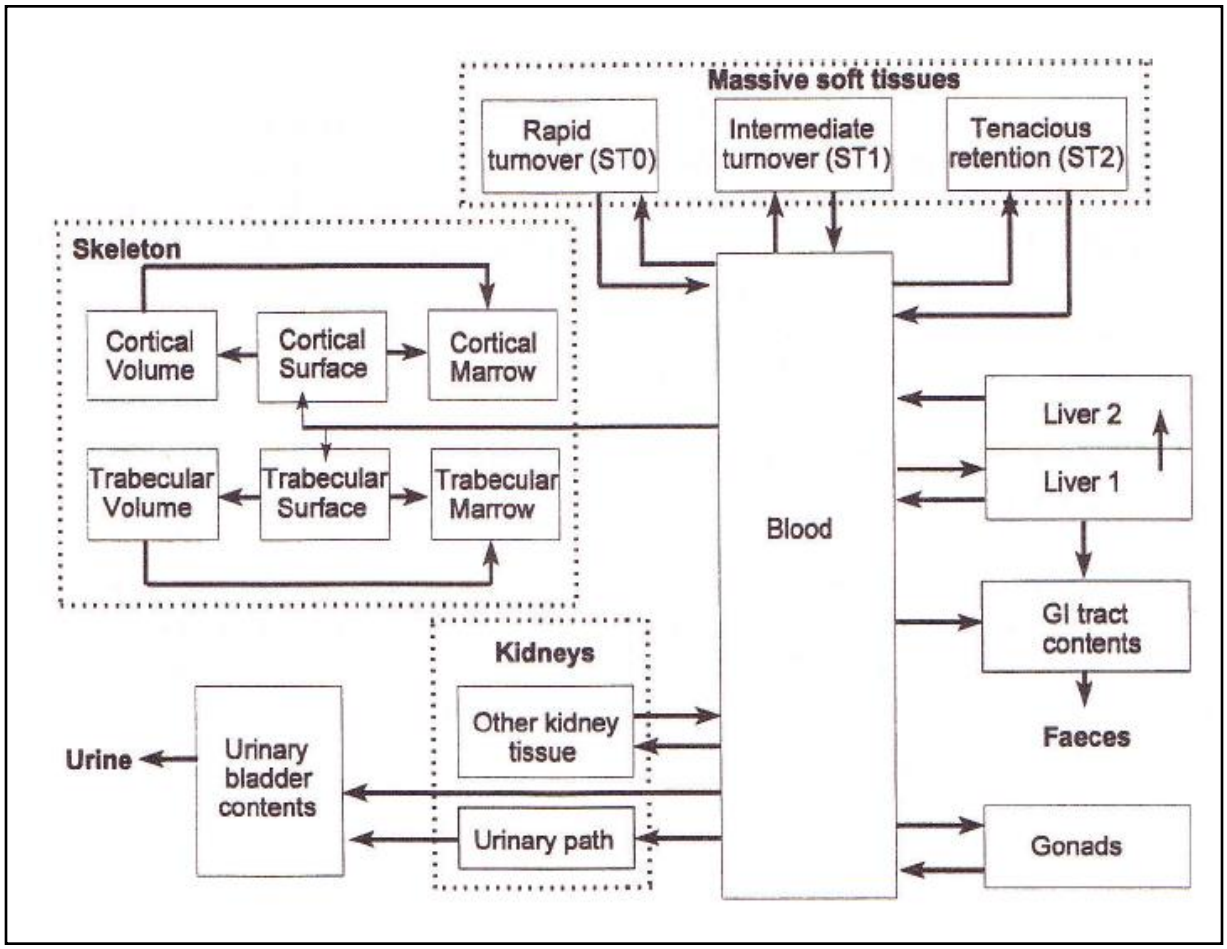

Figure 2.2. Diagram of the biokinetic model for thorium, neptunium, plutonium, americium, and curium (ICRP67 1993)

The skeleton is divided into two different compartments: cortical and trabecular bone. These in turn are divided into three subcomponents including bone surface, bone volume, and bone marrow. The activity of americium is assumed to be transferred from blood (plasma) directly to the bone surface and then to the bone marrow by the process of bone resorption or to bone volume

by bone formation. The bone resorption rate is the movement of americium to the marrow component, while, the bone formation rate is the movement of americium to the bone volume. Activity is transferred from the bone volume to the bone marrow by bone resorption. The removal of activity from the bone marrow to blood takes a period of months. “During growth, bone formation and re-absorption are assumed to occur at different sites within bone: therefore, the rate of removal of americium from the bone surface is approximated by the sum of the bone resorption (represented in the model by movement of americium to the marrow compartments) and the rate of bone formation (represented by movement of americium from the bone surface to the bone volume)” (ICRP67 1993).

The liver in this model is divided in to two compartments; which are liver 1 and liver 2. Liver 1 loses its activity to the gastrointestinal tract, by biliary secretion, and to blood (americium) or to liver 2 (plutonium, neptunium) with a biological half-life of one year. “Kidneys consist of two compartments, one that loses activity to urine and another that returns activity to blood. The urinary bladder content is considered to be a separate pool that receives all materials destined for urinary excretion” (ICRP67 1993).

Massive soft tissues such as muscle, skin, subcutaneous fat, and all others soft tissues not included in other compartments of the model are treated as a mixed pool that includes three compartments. ST0 is used to represent slow retention (hours or days) which exchanges materials with blood and extracellular fluids. ST1 represents intermediate retention (up to two years) and ST2 represents tenacious retention (many years) (ICRP67 1993).

“The model assumes that in adults, 50% of the americium that enters the body and which is not excreted is transferred to the liver and 30% is transferred to the skeleton. The other 20% is assumed to be excreted. Skeleton deposition is assumed to distribute in to two pools: 50% goes to

the trabecular bone surface and 50% to the cortical bone surface. A first order rate coefficient for elimination of americium from liver to plasma is assumed to be 0.0019 day^{-1} (half-time, 356 days)" (ICRP67 1993).

The americium biokinetic model published in ICRP 67 has four recycling pathways to the blood; soft tissues to blood, liver to blood, gonads to blood, and kidneys to blood.

Activity transfer rates into each organ from the transfer compartment (blood) are determined using the assumed deposition fraction on that organ, DF:

Organ Transfer Rate= $\frac{0.693}{T_b} \cdot DF$ (Equation 2)

Where T_b is the overall biological half-time of elimination from the blood and DF is the deposition fraction.

Table 2.3. The default biokinetic parameters that were recommended by the International Commission on Radiological Protection (ICRP67 1993)

Route of Transfer Rate Between Compartments	Transfer Rate (1/d)
Blood to Liver	1.16×10^{1}
Blood to Cortical Surface	3.49
Blood to Trabecular Surface	3.49
Blood to Urinary Bladder Content	1.63
Blood to Kidneys (Urinary Path)	4.66×10^{-1}
Blood to Kidneys (Other Tissue)	1.16×10^{-1}
Blood to ULI[a]	3.03×10^{-1}
Blood to Testes	8.20×10^{-3}
Blood to Ovaries	2.60×10^{-3}
Blood to ST0[b]	1.00×10^{1}
Blood to ST1	1.67
Blood to ST2	4.66×10^{-1}
ST0 to Blood	1.39
ST1 to Blood	1.39×10^{-2}
ST2 to Blood	1.90×10^{-5}
Cortical Volume to Cortical Marrow	8.21×10^{-5}
Cortical Surface to Cortical Volume	4.11×10^{-5}
Cortical Surface to Cortical Marrow	8.21×10^{-5}
Trabecular Volume to Trabecular Marrow	4.93×10^{-4}
Trabecular Surface to Trabecular Volume	2.47×10^{-4}
Trabecular Surface to Trabecular Marrow	4.93×10^{-4}
Trabecular Marrow to Blood	7.60×10^{-3}
Cortical Marrow to Blood	7.60×10^{-3}
Live to Blood	1.85×10^{-3}
Liver to GI Tract	4.90×10^{-5}
Testes to Blood	1.90×10^{-4}
Ovaries to Blood	1.90×10^{-4}
Kidneys (Other Tissue) to Blood	1.39×10^{-3}
Kidneys (Urinary Path) to UBC[c]	9.90×10^{-2}

[a]ULI= Upper Large Intestine.
[b]ST= Soft Tissue.
[c]UBC= Urinary Bladder Content.

2.3.2. NCRP 156 Wound Model

The wound cases included in this dissertation are thought to have experienced chemical and physiological conditions at the wound site that delayed the entrance of the radionuclides into the blood and therefore, they could not be modelled like samples that only needed the systemic model for good predictions, e.g., intravenous administration (NCRP 2006). The entrance of the radionuclides via the wounds is dependent on the physical and chemical properties of the radionuclide, and the depth of the wound. (NCRP 2006). In these cases, the systemic biokinetic model had to be coupled to the wound model to describe the mode of intake into the blood and body.

The ICRP 67 systemic model considers organs as compartments. The NCRP wound model includes seven compartments, five of which explain the wound site. The five compartments are classified based upon the physical and chemical properties of the radionuclide as well as their anticipated retention (Guilmette et al, 2007). The NCRP wound model assumes that the radionuclide is cleared from the wound site by either the lymphatic or vascular system to be either deposited in lymph nodes or to experience systemic uptake from the blood.

The three categories describing the physical particle retention include colloids, particles, and fragments (Table 2.4). According to NCRP Report No.156, fragments are defined as any material with diameter above 20μm, while particles are defined as any material with diameter up to 20μm. Colloid material results from soluble materials that enter the wound and which are immediately transferred to the Colloid and Intermediate State (CIS) compartments, where the materials become hydrolyzed at neutral pH in the tissue fluid and from there are converted from a dissolved solute to a solid phase (NCPR 2007).

Am-241 is classified within NCRP 156 as soluble. Using the soluble radionuclide classification, the generalized wound model may be simplified to three compartments consisting of Soluble, Colloid and Intermediate State (CIS), and Particles Aggregate and Bound State (PABS) compartments as shown in Figure 2.3. Initially, soluble substances are injected into the soluble wound compartment. A fraction of the activity may enter the CIS compartment or be transferred to the blood. In the CIS compartment, some of the activity may return to the soluble state and some of it may be altered by chemical reactions and subsequently transferred into a bound state in the Particles Aggregates and Bound State (PABS) compartment. Finally, the activity remaining in the CIS and PABS compartments is cleared from the wound site by either the vascular or the lymphatic system to be either deposited in lymph nodes or to experience systemic uptake from the blood. The two models are linked together by the blood compartment.

Four categories of retention were defined for radionuclides present in the wound in initially soluble form including Weak, Moderate, Strong, and Avid. The classification depends on the amount of the retained materials in the first day after deposition and the rate for the clearance of the reminder activity Table 2.4.

The NCRP model classified Am-241 (III) as a strongly retained radionuclide, in such situation the retention at the wound site was assumed to be 32 to 85% of the available activity at 1 day and 8 to 40% at 64 days (NCRP 2006).

Wound retention can be expressed by the following multiexponential equation (NCRP, 2007):

$$R(t)_{strong} = 50e^{-1.1t} + 32e^{-0.029t} + 18e^{-0.00086t} \qquad \text{(Equation 3)}$$

Where:

R (t) = radionuclide retention at the wound site (% of material initially deposited)

t = time after deposition (days)

Table 2.5. summarizes the transfer rates among wound model compartments for strongly-retained radionuclides.

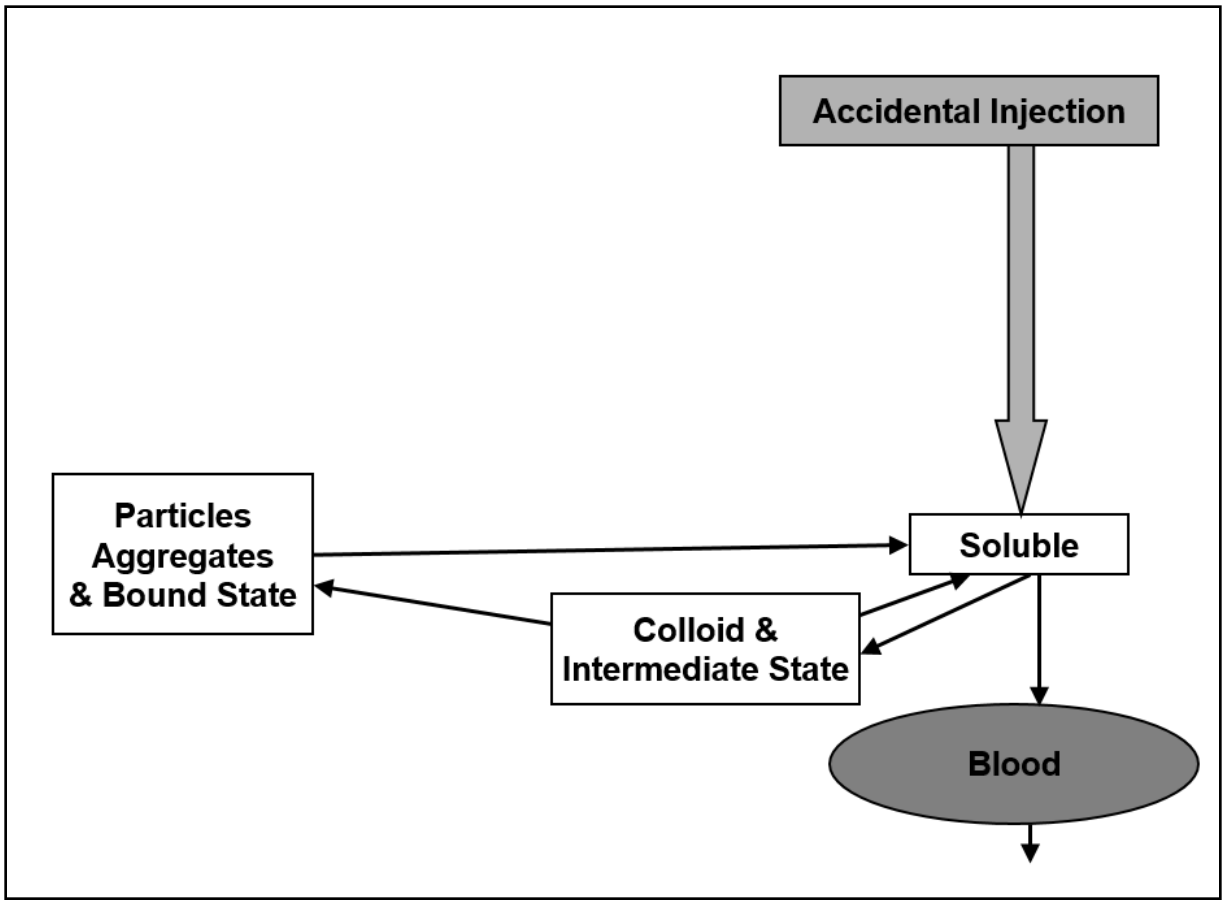

Figure 2.3. NCRP general wound model (NCPR 2007)

Table 2.4. NCRP 156 default transfer rates for different types of physical materials (NCRP 2006).

Pathway	Transfer Rate ($days^{-1}$)						
	Radionuclides initially in solution				Colloids	Particles	Fragments
	Weak	Moderate	Strong	Avid			
Soluble to blood	45	45	0.76	7.00	0.50	100	
Soluble to CIS	20	30	0.60	30.00	2.50		
CIS to soluble	2.80	0.40	2.4×10^{-2}	0.03	2.5×10^{-2}		
CIS to PABS	0.25	6.5×10^{-2}	1.0×10^{-2}	10.00	5×10^{-2}		
CIS to lymph nodes	2×10^{-5}	2×10^{-5}	2×10^{-5}	2×10^{-5}	2×10^{-3}		
PABS to soluble	8×10^{-2}	2×10^{-2}	1.2×10^{-3}	0.005	1.5×10^{-3}	2×10^{-4}	0.00
PABS to lymph nodes	2×10^{-5}	2×10^{-5}	2×10^{-5}	2×10^{-5}	4×10^{-4}	3.6×10^{-3}	0.004
PABS to TPA						4×10^{-2}	0.70
TPA to PABS						3.6×10^{-3}	5×10^{-4}
Lymph nodes to blood				3×10^{-3}		6×10^{-4}	3×10^{-2}
Fragment to soluble							0.00
Fragment to PABS							8×10^{-3}

Table 2.5. NCRP 156 wound model transfer rates for strongly retained intermuscular radionuclides (NCRP 2006).

Pathway	Transfer rate for strongly retained intermuscular radionuclides (d^{-1})
Soluble to blood	0.67
Soluble to CIS	0.60
CIS to soluble	0.024
CIS to PABS	0.001
CIS to lymph nodes	0.00002
PABS to soluble	0.0012
PABS to lymph nodes	0.00002

2.3.3. Pattern of Distribution, Retention, and Excretion Observed in Beagle Dogs and Baboons Post Injection With ^{241}Am Citrate

Several experiments were conducted to evaluate the metabolism of americium using different kinds of animals. Lloyd et al. (1970) studied the retention of ^{241}Am activity in liver, skeleton, and other soft tissues in beagle dogs following its intravenous administration. These animals were injected with 66 to 166,000 Bq ^{241}Am/kg body mass. The results reported in that study showed fluctuation in liver and skeleton retention depending on the level of injected dosage. The authors showed that the principal sites of activity retention in beagle dogs, were liver and skeleton (Lloyd et al. 1970). Rosen et al. (1972) and Guilmette et al. (1989) also investigated ^{241}Am translocation in baboons after intravenous administration. In these studies both authors described the distribution, retention, and excretion of injected ^{241}Am in these nonhuman primates (NHP). It was observed that the majority of soluble ^{241}Am in baboons was transferred and deposited in the liver and skeleton in the first day. In addition, urine excreta contained the most activity during the first week, whereas fecal excreta dominated after the first week (Rosen et al. 1972, Guilmette et al. 1980).

2.3.4. ICRP 67 Biokinetic Model for Am-241 Applied to Nonhuman Primates

Alomairy et al. (2017) studied the predictions of ICRP 67 for ^{241}Am translocation and excretion in NHP using the data generated in the Durbin studies (Durbin et al. 1990). Seven cases, in which the primates were administrated ^{241}Am citrate by intravenous injection were used. One case wasexcluded from analysis because it has lack of enough data to include in the study. They observed that the ICRP 67 biokinetic model frequently predicted the observed excretion well. However, the fits of the ICRP 67 model were questionable when considering data from the animals sacrificed more than 100 days after injection. The excretion data for two of the six monkeys

compared well with the default biokinetic model resulting in P-values greater than 0.05 for both chi-squared and autocorrelation “see materials and methods”; these data sets arose from animals sacrificed soon after injection (less than 100 days). Data from the other four monkeys sacrificed after a long period of time (more than 100 days) was not well explained using the default parameters. The difference between the intake predicted using urine bioassay data and the actual intake ranged from 51.4% underestimated activity to 102.7% overestimated activity. Predictions of organ activity were compared to measured organ activities at the time of death, and ranged from nearly perfect to 30 times overestimation in the liver. The skeleton predictions ranged from 1.14 times greater than measured to 0.89 times less than measured values, which were reasonably in agreement (Alomairy et al. 2017).

Alomairy et al. (2017) developed sets of new transfer rates for the individual NHP that improved the fits and, predicted the intakes and organ activities better than the ICRP 67 default model (Table 2.6). The new parameters in most cases adequately described Am systemic distribution in the Durbin monkeys. Although a new set of optimized transfer rates among compartmentalized organs was obtained, the predicted intake did not improve substantially with the optimized parameters even though an adequate model fits were observed in every case. Nor was the predicted activity retained in skeleton or liver substantially improved when the optimized parameters were used. It is noted in most cases, that the predicted activity using default parameters in the skeleton or liver become increasingly larger than the measured values as the time after injection increased. The discrepancy between the predicted and measured activities is hypothesized to due to the differences in biokinetic and life expectancy between humans and NHPs (Alomairy et al. 2017).

Table 2.6. The modified transfer rates using the posterior probability distribution for each case

		Optimized Transfer Rates						
Route of TR between Compartments	**Default TR (1/d)**	**C41F**	**C42F**	**C72F**	**C73F**	**C75F**	**C76F**	**GSD**
Blood to ST0	1.00×10^{1}	5.1×10^{1}	3.00×10^{1}	2.9×10^{1}	2.9×10^{1}	1.65×10^{2}	1.953×10^{2}	1.5
Blood to ST1	1.67	2.67	4.39	4.87	4.87	1.668×10^{2}	1.701×10^{2}	1.5
Blood to ST2	4.66×10^{-1}	2.17×10^{-1}	1.85×10^{-1}	1.35	1.35	2.36×10^{2}	1.99×10^{2}	1.5
ST0 to Blood	1.39	4.89	1.66	3.65×10^{-3}	3.65×10^{-3}	1.386	1.386	1.5
ST1 to Blood	1.39×10^{-2}	2.53×10^{-4}	2.04×10^{-3}	7.33×10^{-5}	7.33×10^{-5}	1.39×10^{-2}	1.39×10^{-2}	1.5
ST2 to Blood	1.90×10^{-5}	4.45×10^{-10}	3.14×10^{-10}	4.01×10^{-10}	4.01×10^{-10}	*1.9×10^{-5}	1.9×10^{-5}	1.5

TR= Transfer Rate

Chapter 3:

Materials and Methods

3.1.Lawrence Berkeley Laboratory Experiment

At Lawrence Berkeley National Laboratory, researchers recognized the importance of studying rhesus and cynomolgus macaques. Therefore, these animals were exposed to different kinds of radioactive materials with a known intake (Durbin et al. 1993a and b). Rhesus monkeys are one of the most broadly used NHP used for study since they are more similar to humans than other types of animals that are used as research surrogates for humans (Gibbs et al. 2007).

Americium kinetic studies in monkeys were started in 1960 because of a lack of available metabolic data. Between 1960 and 1985, several studies were conducted by P.W. Durbin et al. on NHPs. Animals were injected intravenously or intramuscularly with isotonic sodium citrate $^{241}Am(NO_3)_3$ at doses ranging from 16 to 32 kBq kg^{-1} [1] (Table 1.1). These experiments were conduct at the Division of Research Medicine and Radiation Biophysics, Lawrence Berkeley National Laboratory.

As part of the experimental design, urine and feces were collected and blood samples were taken at various intervals post injection up to death. The subjects were sacrificed at various times ranging from 1 day to 2,199 days after injection for further analyses. An autopsy was performed on each animal; thus, all soft tissues and bones were removed, weighed and radioanalyzed for americium content. The absolute amount of ^{241}Am injected into each monkey was obtained by

[1]The solution was provided by the Actinide Chemistry Group at Lawrence Berkeley National Lab in 1960.

counting the alpha activity using a windowless proportional counter and dual crystal scintillation detection systems (Durbin et al. 1990).

Since nonhuman primates are phylogenetically the closest animals to humans, data generated from experiments using these animals may be relied upon. However, they are not humans and subtle differences are known to exist. Therefore, it is extremely important to analyze the Durbin data with the intent of comparing results with those from other experimental animals as well as available human data.

The Durbin monkeys were treated with intramuscular (i.m.) or intravenous (i.v.) injections of Am-241 isotonic sodium citrate $^{241}Am\ (NO_3)_3$ at doses of 16 to 32 kBq kg^{-1} . The solution was provided by the Actinide Chemistry Group at Lawrence Berkeley National Lab in 1960 (Durbin et al, 1990). ^{241}Am isotonic sodium citrate solution was stored at $4\,^0C$ and diluted with isotonic sodium citrate in a serum bottle (from 1 to 5 mL volume) using a calibrated syringe. The absolute amount of Am-241 injected into each monkey was obtained by counting the alpha activity in aliquots of each counting standard using a windowless proportional counter (Durbin et al. 1990).

All the animals lived in the LBL (Lawrence Berkeley National *Laboratory*) colony in separate cages after their arrival. From 1960 to 1970, monkeys were kept in metabolic cages (0.53m tall, floor area $0.20m^2$) constructed from iron sheet metal that were used to collected feces. After 1970, animals were transferred into different cages (0.7 to 0.9m high with floor areas from 0.37 to $0.65m^2$) according to their sizes (Durbin et al 1990).

Monkeys were given fresh vegetables and fruits, iron and vitamins, dry biscuits and reconstituted fortified milk. From 1960 to 1970, infant monkeys were given enriched bread and biscuits (Durbin et al, 1990). Initially before 1963, monkeys were bought in bulk quantity and were sent to buyers without complete isolation. Initially when monkeys were brought to LBL, they

were housed in a quarantine room and were treated for intestinal worms with oral vermifuges. After 1963, monkeys were imported in smaller quantities and were held in isolation for several months so that they could be brought to good health. As the time passed, housing standards, cleanliness and care were improved (Durbin et al. 1990).

There were two types of injections used. The intravenous injections (i.v.) were made into the superficial veins of the animal's calf and ankle; intramuscular injections (i.m.) were made into the thickest part of the thigh (proximal thigh). The medical history maintained for each monkey included results of TB tests, body weights, any surgical procedures, and treatment of infections (Durbin et al. 1990). Before 1970, excreta collection from the cages at LBL involved removal of solid matter from the pull-out small mesh screen, and rinsing the funnel-shaped urine collecting unit beneath the cage into the attached urine-collecting jar, wiping up any residues and adding them to the jar. To make a collection, the pan and screen were removed from beneath the cage, and a catch pan was inserted under the cage to collect any excreta passed during the cleaning of the pan and screen. The feces screen was lifted out of the pan and transferred to a clean pan lined with large tissues. Lumps of feces that have fallen into the urine pan were picked up with tweezers and transferred to the feces screen. Food scraps, which were assumed to have been possibly contaminated by urine, were picked out of the urine pan from the feces screen with tweezers and put into the urine collection beaker (Durbin et al. 1990).

A complete mass balance study was performed for each Americium injected monkey. This Am content was determined for all the bones, excreta, blood samples, i.m. injections and tissues, and these results were summed. Due to the incomplete collection of excreta and errors in measurement of injected activity, 100% recovery of the materials could not be achieved. The measurements of the injected activity were normalized to 100% using the following equation:

NF = 100% ID/ (%ID in tissues, bones, excreta - % ID in blood samples) (Equation 4)

where, %ID is the percentage of injected dosage

It should be noted that 100% of injected Am was not recovered. This loss in the total Americium content was thought to be associated with counting standards that had potential errors that were likely experienced when combining the different measurements of the amount of Am injected. They also include systematic errors in radioanalysis of the sample. Therefore, samples such as bones, tissues, and excreta were corrected by a normalization factor for every monkey. Nevertheless 99.57% of the percentage of the injected dosage (ID) was the average material recovery for the 30 monkeys, which gave some assurance regarding the overall validity of the excreta collection procedure and on the radioanalytical procedure (Durbin et al. 1990).

Blood samples were taken regularly on an a *priori* basis. This was done to measure plasma clearance kinetics. In this procedure, small samples (1 to 3 ml to minimize blood loss) were taken many times; twice a day for 3 to 4 days starting between the first 6 to 8 hours. This process continued for at least 2 weeks. About twice a year, (3 to 10 ml) volumes of blood were taken from every animal in the colony so that normal hematological examinations could be performed. The Am content of blood was also obtained from these samples. The quantity of the blood volumes obtained were determined by gravimetric means.

To sacrifice these animals, they were given an overdose of Ketelar, Diabutal, and Sernylan Nembutal. Their abdomens were opened after death. The abdominal and thoracic organs were removed, dissected cleanly, examined and weighted. After examination, for the purpose of ashing and drying, the dissected organs were placed in beakers of appropriate sizes. Tissue sample were also taken with the intention of histological examination and autoradiography. All such samples

were weighted and their Am-241 content was assessed, making these data available for mass balance efforts.

Gastrointestinal contents were removed, rinsed and bottled. GI contents were in this way added to the last fecal collection. The feet were removed from the legs of the i.m injected monkeys. Hip joints were analyzed intact and processed. Analysis was completed on the defleshed bones, muscle, and skin of uninjected leg of these monkeys. This was treated as separate samples. The carcass of injected animals was skinned an all subcutaneous fats was removed from the pelt. Any remaining tissues were collected.

During dissection of the skeleton, connective tissue, fats, and muscles were dried, ashed and weighted prior to radioanalysis (Durbin et al, 1990). A standard set of defleshed bone samples were weighed bone samples was preserved in 80% ethanol prior to obtaining autoradiographs. Defleshing the bones of a monkey usually required 2 to 3 working days to complete (Durbin et al. 1990).

The wrists and hands bones, ankles and feet bones and the cervical, thoracic, and caudal vertebrae (tail) were not easy to deflesh completely, these were roughly cleaned without disarticulation. The teeth were removed from the skull and mandible after ashing (Durbin et al. 1990).

Excreta, bone, and tissues were dried at 100 to 200 °C. Those beakers which contained mesentery, skin, and dried muscles were weighted. To determine the mass of surplus fat, the beakers were reweighed after separating fat. Analysis and ashing was separately done on fat samples taken from Am-injected monkeys. It was found that there was no radioactivity in the fat so after separation, ultimately the fat was discarded.

A furnace was used for ashing. Samples were ashed at a temperature of 600°C. Samples were ashed until they were substantially reduced in volume and turned grey. The large soft tissues and excreta in addition to being dry-ashed were digested to produce a carbon-free salt using concentrated H_2O_2 and HNO_3 (Durbin et al. 1990).

There were two systems used for the detection of either photons or alpha particles emitted by Am-241. The system used for detecting alpha particles was a Nuclear Chicago proportional counting system. The counting efficiency for alpha particles with 5.5-MeV was around 45% on glass planchets and 32% on steel planchets in flat films. "Background was about 1.5 counts/ min; replacement of a preamplifier several years into the project reduced the background to about 0.4 count/ min. After 1970, a custom built dual-crystal scintillation detection system was used to count the photons emitted by Am-241 in all biological samples containing more than about 0.05% of the injected radioactivity (Durbin et al. 1990)". To accomplish photon analysis, samples were suspended in diluted HNO_3 and both stored and counted in plastic bottles.

A large single NaI(TI) crystal, and an Anger whole-body scanner were used in order to obtain *in vivo* measurements of the Am-241 content. The whole body distribution of americium in these animals was evaluated using an Anger whole body scanner attached to a fixed overhead gamma ray detector with moving bed (Durbin et al. 1990). A *large* single NaI(TI) crystal (1 0-cm thick and 24 cm in diameter) was used to measure the body content of monkeys injected with ^{241}Am.

All teeth were extracted wet from the skull and mandible of three monkeys at autopsy. The extracted teeth were weighed wet and ashed. The tooth roots were carefully removed from the ashed bone (the crowns usually separated during ashing and fell to the bottom of the ashing beaker) (Durbin et al. 1990).

3.2. Methods for Analysis of Bioassay Data

To compare the intake from the bioassay data, several methods have been described in the literature. One of the simplest methods to calculate the intake is to use the intake retention fraction or the excretion fraction which is given as (IAEA 2004):

$$I = \frac{M(t)}{m(t)}$$

where, *M(t)* is the measured body content, body region content or excretion rate at time *t*, and *m(t)* is the fraction of unit intake retained in the whole body or in body organs (intake retention fraction (IRF)) or the amount excreted in a time period from the body at time *t* (intake excretion fraction). This method is useful when evaluating one data point.

Another common approach is to use the least square method. This method is used when more than one data point available in order to avoid the inherent uncertainty in estimating the intake from a single bioassay measurement. The least square method basically minimizes the sum of the squares of the deviations *S* of the observed measurements from the model predictions.

$$S = \sum_i \left[M_i - I \quad m(t_i) \right]^2$$

The best estimate of intake *I* is given as (USNRC 1987, IAEA 2004):

$$I = \frac{\sum_i M_i m(t_i)}{\sum_i m(t_i)^2}$$

where, *m(ti)* is the intake retention fraction associated with the *i*th measurement and *Mi* is the value of the *i*th measurement.

A weighted least squares fit method is recommended and used by most authors. In this method, the bioassay data point is essentially weighted by certain much factors to obtain a better

estimate of the intake. (Skrable et al. 1988, IAEA 2004). Using the weighted least squares fitting method, the best estimate of intake *I* is given as:

$$I = \frac{\sum_i \left[M_i \quad m(t_i) w_i \right]}{\sum_i \left[m(t_i)^2 w_i \right]}$$

where *wi* is the weighting factor based on either the information on the error associated with each measurement or on the subjective assessment of confidence in each data point or data set. This method minimizes the sum of the squares of the deviation *S* where,

$$S = \sum_i \left[M_i - I \quad m(t_i) w_i \right]^2$$

The most commonly used method for hypothesis testing is the maximum likelihood method (IAEA 2004, Doerfel et al. 2006, 2012). This method is commonly used for estimating the parameter(s) of a statistical model from a sample data set (Cam 1990). The IMBA software uses the maximum likelihood method as its default bioassay data fitting routine. The method determines a best estimate of intake (I) from a set of up to 200 bioassay data $m_i(t_i)$, where m(t) represents an excretion or retention data point as a function of time. M_i is measured bioassay data, and SF_i is the scattering factor for M_i. The best fit is obtained by achieving the minimum uncertainty-weighted value of (χ^2) using the following equation (James 2005; Castellani el al. 2013).

$$\chi^2(I) = \sum_{i=1}^{n} \frac{\left[\ln(M_i) - \ln(\mathrm{I}\, m(t_i)) \right]^2}{\left[\ln(SF_i) \right]^2}$$

3.3.Uncertainties in Bioassay Measurements

Each bioassay measurement is associated with statistical or non-statistical errors and uncertainties (Type A and Type B errors) (BIPM et al. 2010). A type "A" error is the random error due to the nature of radioactive decay and can be characterized by using a Poisson distribution (Hurtgen and Cossonnett. 2003, Castellani et al. 2013). The Type "B" errors are the systemic errors due to other error in measurements. Examples of Type "B" errors are the measurements of sample volume or weight, chemical yield, electronic stability, contamination of sample and impurities, source positioning for counting, counting efficiency, counting time, and background measurements (Hurtgen and Cossonnett 2003, Castellani et al. 2013). Similarly, Type B errors may be due the results of counting geometry errors, positioning or movement of the individual, differences between phantom and individual or organ, variations in background radiation, external contamination of the person, uncertainties in calibration source, etc. (Castellani et al. 2013).

The assessment of the uncertainties is important when calculating the intake because it allows one to properly estimate the intake and calculate the chi-square which can be used to compare the consistency of the model with the data.

According to the IDEAS guidelines, the scattering factor or the geometric standard deviation (SF) is assumed to be a log-normal distribution of measurement uncertainty. If *SFA* and *SFB* are the scattering factors for type A and B errors corresponding to the counting and "other" uncertainties respectively, the total scattering factor, *SF*, is then;

$$SF = \exp\sqrt{[\ln(SF_A)]^2 + [\ln(SF_B)]^2}$$

The analysis of several bioassay samples and their uncertainties in literatures indicate the scattering factor B dominates the calculation over scattering factor A, and hence the IDEAS

guidelines adopted the *SFB* as the overall *SF* in the bioassay measurements (Doerfel et al. 2006, 2012; Castellani et al. 2013).

Based upon the IDEAS guidelines, the scattering factor is characterized by geometric standard deviation that was assumed to be 1.6 for simulated 24-h urine samples and 3 for fecal bioassay samples. These values as recommended with the IDEAS documentation were used for the purpose of this dissertation (James 2005; Castellani et al. 2013).

3.4. Integrated Modules for Bioassay Analysis (IMBA)

To achieve the objectives of evaluating the applicability of the ICRP 67 standard biokinetic model for americium and the recommended transfer rates as applied to NHP, a special academic version of Integrated Modules for Bioassay Analysis (IMBA), called IMBA Professional Plus was used[2]. The software used the latest recommended biokinetic and dosimetric models for americium to estimate excretion or other bioassay predictions following a known intake. IMBA also allows the user to estimate the most likely intake from a set of bioassay measurements, and calculate bioassay quantities or doses from a hypothetical intake (Birchall et al. 2006).

IMBA allows users to load default dosimetric and systemic compartmental models such as the ICRP 30 gastrointestinal tract model and the ICRP 66 lung model and solve these in conjunction with the entered bioassay and health physics data. IMBA is used to compute intake and doses from bioassay measurements received based on either whole body count or *in vitro* excretion measurements. This is accomplished by implementing the current internationally acceptable biokinetic and dosimetric models.

[2] Radiation Protection Division of the Health Protection Agency (HPA, currently Public Health England), UK.

A statistical maximum likelihood chi-square test (χ^2) at the 95% confidence interval ($P \succ 0.05$) indicates a "good" fit to the data and the minimized chi-square situation for each case considered provides an estimate of the *optimum* fit. The chi-square statistic describes the goodness of fit to a set of data by measuring the disparity between observed data points and the predicted curve. A zero chi-square value is possible when the expected data points perfectly correspond to the predicted function. However, a perfect match is highly unlikely considering measurement error. The parent distribution and the experimental distribution match is maximized by minimizing the sum of (χ^2).

The autocorrelation coefficient is another statistic used to assess the goodness of fit of biokinetic models to bioassay data, and therefore, used to detect non-random scatter bias around the fit. The autocorrelation coefficient (ρ) for a sequence of residuals is defined based upon the following equation (Puncher 2007):

$$\rho = \frac{\sum_{i=1}^{N-1} R_i R_{i+1}}{\sum_{i=1}^{N} R_i^2} \qquad \text{(Equation 6)}$$

where:

N= the number of residuals ($N \geq 4$)

R_i = the ith residual of N residual

ρ = is a value between -1 and 1.

For a lognormal distribution, each residual is defined based upon the following equation:

$$R_i = \frac{\ln(M_i) - \ln(\mathrm{Im}(t_i))}{\ln(\sigma_g)} \qquad \text{(Equation 7)}$$

where:

$\ln(M_i)$ = The ith measurement, made at time t_i after the intake.

I= the estimated intake.

$m(t_i)$= A fraction given the relevant bioassay quantity, for a unit intake, at time *ti* after the intake.

σ_g = the geometric standard deviation assumed to represent the uncertainty of the data.

The autocorrelation coefficient is likely to be close to zero in totally random conditions and a ρ close to 1 or -1 means a less random scatter of data points around the fitted function. This statistic can expose a poor model fit to data resulting from non-randomness in bioassay data residuals and has been found to be an effective tool in bioassay analysis. The autocorrelation test provides a more stringent evaluation of the fit to the case data than the chi-square test alone (Puncher et al 2006).

Using IMBA Professional Plus, we examined the applicability of the ICRP default models and

parameters to the Durbin primate cases by trying to obtain the best "goodness-of-fit" to the primate bioassay data. The main screen of IMBA is shown in Figure 3.1.

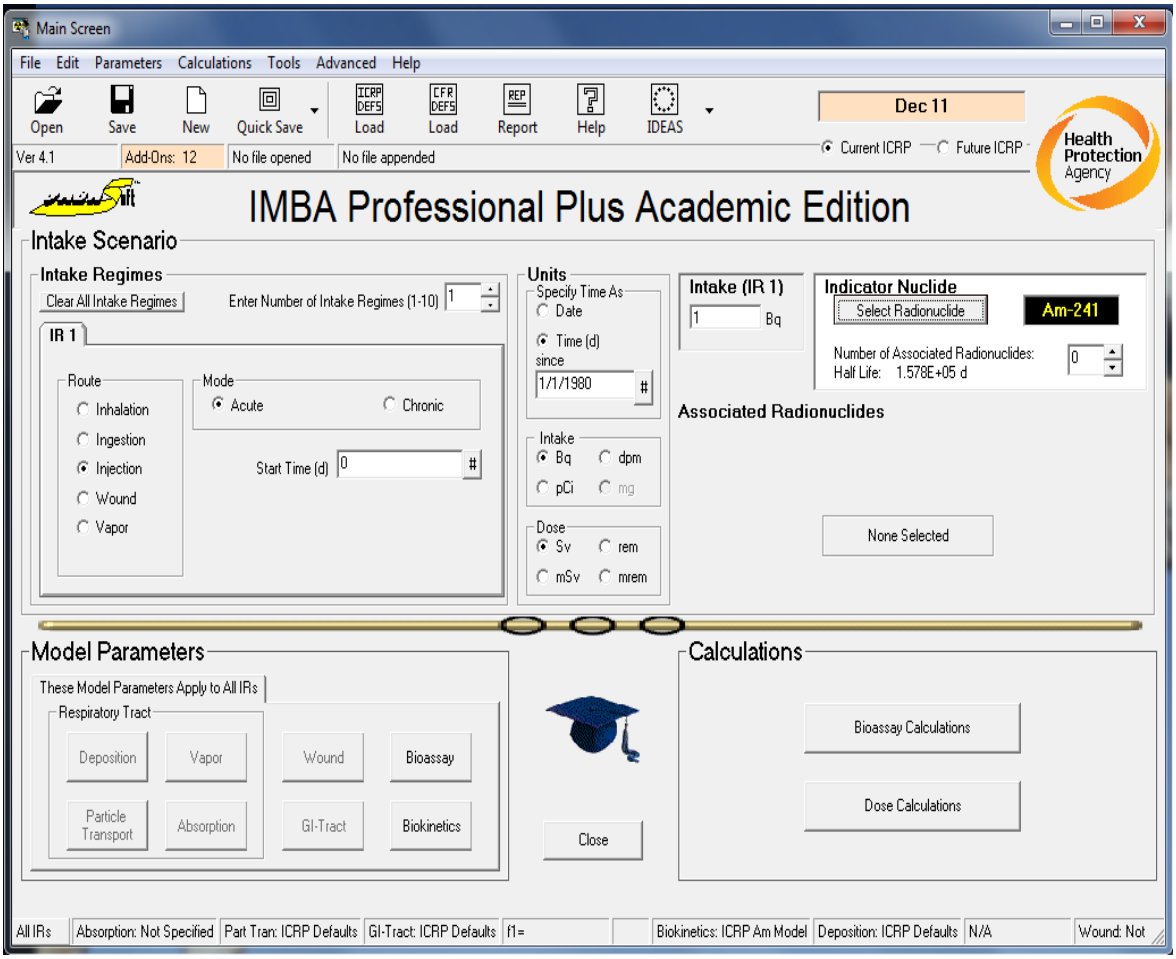

Figure 3.1. The main screen of IMBA

3.5.IMBA Uncertainty Analyzer

Based upon bioassay information resulting from the americium uptake in nonhuman primates, the default transfer rates published in ICRP 67 were used to predict the known intake and organ activity at the time of death in the Durbin NHP subjects. These values were also used to determine an adjusted set of a new transfer rates in attempt to improve the fit of the model based upon the nonhuman primates data.

IMBA has a companion program called IMBA- Uncertainty Analysis (UA). This was developed for research purposes by the Health Protection Agency (Puncher, Birchall, 2007). IMBA-UA applies a Bayesian approach to calculate uncertainties of doses from bioassay data and provides the distribution of the mean value using the same techniques. One may obtain the distribution for transfer rates associated with various ICRP systematic models based upon excretion, intake, and postmortem organ activities.

The software was used to estimate parameter values that best fit the data and the associated uncertainty. These values represent the best possible value because they incorporate knowledge of *a priori* distributions and that of measured data. This uncertainty in the estimate of these values is defined using an *a posterior* probability distribution. The *a posterior* distributions of interest in internal dosimetry include the distributions of dose, biokinetic parameter values, intakes, and times of intakes (Puncher and Birchall 2008).

It estimates the overall uncertainty taking into account uncertainties in measurement data and various parameter values. It generates random samples from the *prior* distribution and then uses the sampled values to calculate the most likely values in the posterior density function. This posterior distribution can be established by assigning a weight to each vector equivalent to its

likelihood or by evaluating how well the sampled intake and various modeled parameters fit the data.

The IMBA-UA works by making calls to the required subroutines in the IMBA Professional Plus code. The IMBA Uncertainty Analyzer was originally developed for estimating uncertainties in dose assessments. Special versions of IMBA Professional Plus linked with IMBA UA were developed to estimate doses and bioassay prediction parameters. The software gives users an option of sampling the parameter vectors and calculates the following variables (Puncher and Brichall 2008):

- Bioassay predictions for a unit of intake at the time of the measurement;
- Dose per unit intake for the target organs of interest;
- The Maximum posterior probability of intake;
- The goodness-of-fit-α-probability;
- The $\chi^2 - Statistic$.

The main screen of IMBA-UA is shown in Figure 3.2.

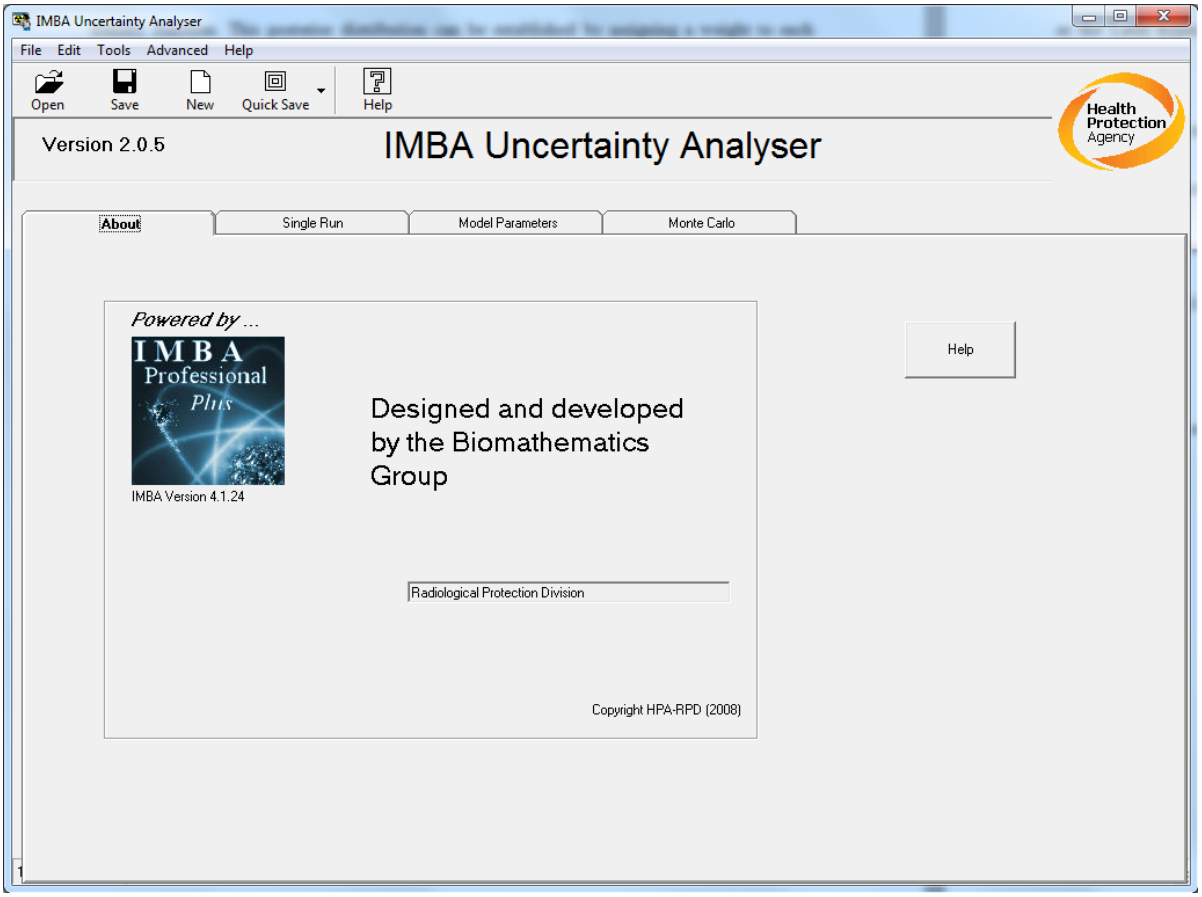

Figure 3.2. The main screen of IMBA-UA

Chapter 4:

Results and Discussion

4.1.Comparison between the Intramuscularly Injected Nonhuman Primates Predications and the predictions made based on ICRP 67 Model and NCPR 156

Twenty animals administered intermuscular injections of ^{241}Am-citrate were sacrificed from 1 to 1,037 days after injection. The default biokinetic parameters recommended by the ICRP 67 and NCRP 156 shown in Table 2.4 and 2.5 were used in IMBA as a benchmark for data comparison. With IMBA software, an evaluation of the efficacy of the default biokinetic parameters to fit the urine and feces, and combination of urine and feces excretion data was completed. The maximum likelihood method chi-squared (χ^2) test was used to evaluate the goodness of fit. When P-values were greater than 0.05, it was concluded that the fit was consistent with the model.

The profile of the urine excretion function is well described by the reference models for human Figure 4.1 (a,b). Acceptable fits (P> 0.05) were obtained for 15 out of 20 monkey cases using urine data only (Table 4.1). Default parameters overestimated the injected activity in 12 cases and the estimated values ranged from 1.01 to 4.41 times the true injected activity from Durbin's data. However, the reference models under-estimated the injected activity in 8 cases, with values that ranged from 0.41 to 0.96 times the actual injected activity. The intake amount was poorly predicted when feces data only were used. The predicted activities ranged from 5.22 to 153.73 overprediction times the measured values (Table 4.2 and Figure 4.2 a&b). When urine and feces excretion data were combined to predict the intake using biokinetic default parameters, unacceptable fits were produced in all cases as indicated by the chi-square test. The injected activities in these situations were overestimated by factors from 1.54 to 9.93 times the true injected value (Table 4.3).

Table 4.1. Comparison between the estimated activities and the actual injected activities using urine data and the maximum likelihood method in IMBA.

Case[a]	Days from injection to death	Estimated Intake (Bq)	Estimated Intake / Injected Intake	P-value[b] (Chi-square)	P-value (Autocorrelation)
C155F	8	3.70×10^4	1.13	**0.99**	**0.29**
C138F	8	7.47×10^4	0.73	**0.93**	**0.55**
C55F	21	7.36×10^4	1.18	**0.99**	**0.61**
C6F	31	7.70×10^4	1.62	**0.71**	**0.23**
C44F	42	7.47×10^4	0.96	**0.56**	**0.06**
C56F	63	7.33×10^4	4.41	0.00	0.00
C146M	64	2.00×10^4	0.76	**1.00**	0.02
C81F	81	7.47×10^4	0.41	**0.11**	0.00
C162F	102	1.18×10^4	1.01	**1.00**	**0.62**
R189M	110	5.81×10^4	1.29	**1.00**	0.00
C157F	156	1.96×10^4	1.32	**0.98**	0.00
C158F	211	1.96×10^4	0.56	**1.00**	0.04
R118M	223	1.21×10^5	1.31	**1.00**	0.05
C57F	224	7.33×10^4	3.84	0.00	0.00
C110F	226	3.66×10^4	0.99	**0.86**	0.00
C156F	301	1.96×10^4	1.26	**0.98**	0.00
C45F	336	7.33×10^4	1.22	0.00	0.00
C46F	735	7.47×10^4	0.75	0.01	0.00
C54F	938	7.40×10^4	1.83	0.01	0.00
C78F	1,037	5.44×10^4	0.7	**0.54**	0.00

[a]M= male, F= female

[b]P-values > 0.05 indicates adequate fits (indicated in bold).

Table 4.2. Comparison between the estimated activities and the actual injected activities using feces data and the maximum likelihood method in IMBA.

Case[a]	Days from injection to death	Estimated Intake (Bq)	Estimated Intake/ Injected Intake	P-value[b] (Chi-square)	P-value (Autocorrelation)
C155F	8	1.00×10^{6}	27.03	**0.17**	**0.10**
C138F	8	5.56×10^{6}	74.38	0.00	**0.59**
C55F	21	3.86×10^{6}	52.42	**0.68**	**0.67**
C6F	31	4.02×10^{5}	5.22	0.00	0.01
C44F	42	1.00×10^{6}	13.39	**0.20**	0.05
C56F	63	3.99×10^{6}	54.38	**1.00**	**0.21**
C146M	64	1.40×10^{6}	69.85	**0.47**	0.03
C81F	81	1.06×10^{6}	14.2	**0.99**	**0.07**
C162F	102	1.81×10^{6}	153.73	**0.99**	0.03
R189M	110	3.79×10^{6}	65.27	**0.74**	0.00
C157F	156	1.26×10^{6}	64.34	**1.00**	0.00
C158F	211	9.02×10^{5}	46.03	**1.00**	0.00
R118M	223	4.25×10^{6}	35.09	**1.00**	0.01
C57F	224	2.13×10^{6}	29.06	**0.54**	0.00
C110F	226	6.20×10^{5}	16.93	**0.60**	0.00
C156F	301	9.77×10^{5}	49.85	**1.00**	0.00
C45F	336	1.00×10^{6}	13.64	0.00	0.00
C46F	735	1.04×10^{6}	13.87	0.00	0.00
C54F	938	1.61×10^{6}	21.72	**0.86**	0.00
C78F	1,037	9.09×10^{5}	16.7	**1.00**	0.00

[a]M= male, F= female

[b]P-values> 0.05 indicates good fit to the data (indicated in bold face).

Table 14.3. Comparison between the estimated activities and the actual injected activities using combined urine and feces data and the maximum likelihood method in IMBA.

Case[a]	Days from injection to death	Estimated Intake (Bq)	Estimated Intake/ Injected Intake	P-value[b] (Chi-square)	P-value (Autocorrelation)
C155F	8	1.14×10^{5}	3.07	0.00	0.00
C138F	8	1.74×10^{5}	2.33	0.00	0.00
C55F	21	2.25×10^{5}	3.06	0.00	0.00
C6F	31	1.68×10^{5}	2.18	0.00	0.00
C44F	42	1.53×10^{5}	2.05	0.00	0.00
C56F	63	6.08×10^{5}	8.29	0.00	0.00
C146M	64	4.75×10^{4}	2.38	0.00	0.00
C81F	81	7.42×10^{4}	9.93	0.00	0.00
C162F	102	4.20×10^{4}	3.56	0.00	0.00
R189M	110	2.01×10^{5}	3.45	0.00	0.00
C157F	156	6.88×10^{4}	3.51	0.00	0.00
C158F	211	3.30×10^{4}	1.68	0.00	0.00
R118M	223	3.62×10^{5}	2.99	0.00	0.00
C57F	224	4.68×10^{5}	6.38	0.00	0.00
C110F	226	7.38×10^{4}	2.02	0.00	0.00
C156F	301	6.24×10^{4}	3.18	0.00	0.00
C45F	336	1.92×10^{5}	2.62	0.00	0.00
C46F	735	1.17×10^{5}	1.56	0.00	0.00
C54F	938	2.52×10^{5}	3.41	0.00	0.00
C78F	1,037	8.39×10^{4}	1.54	0.00	0.00

[a]M= male, F= female

[b]P-values> 0.05 indicates good fit to the data (indicated in bold face).

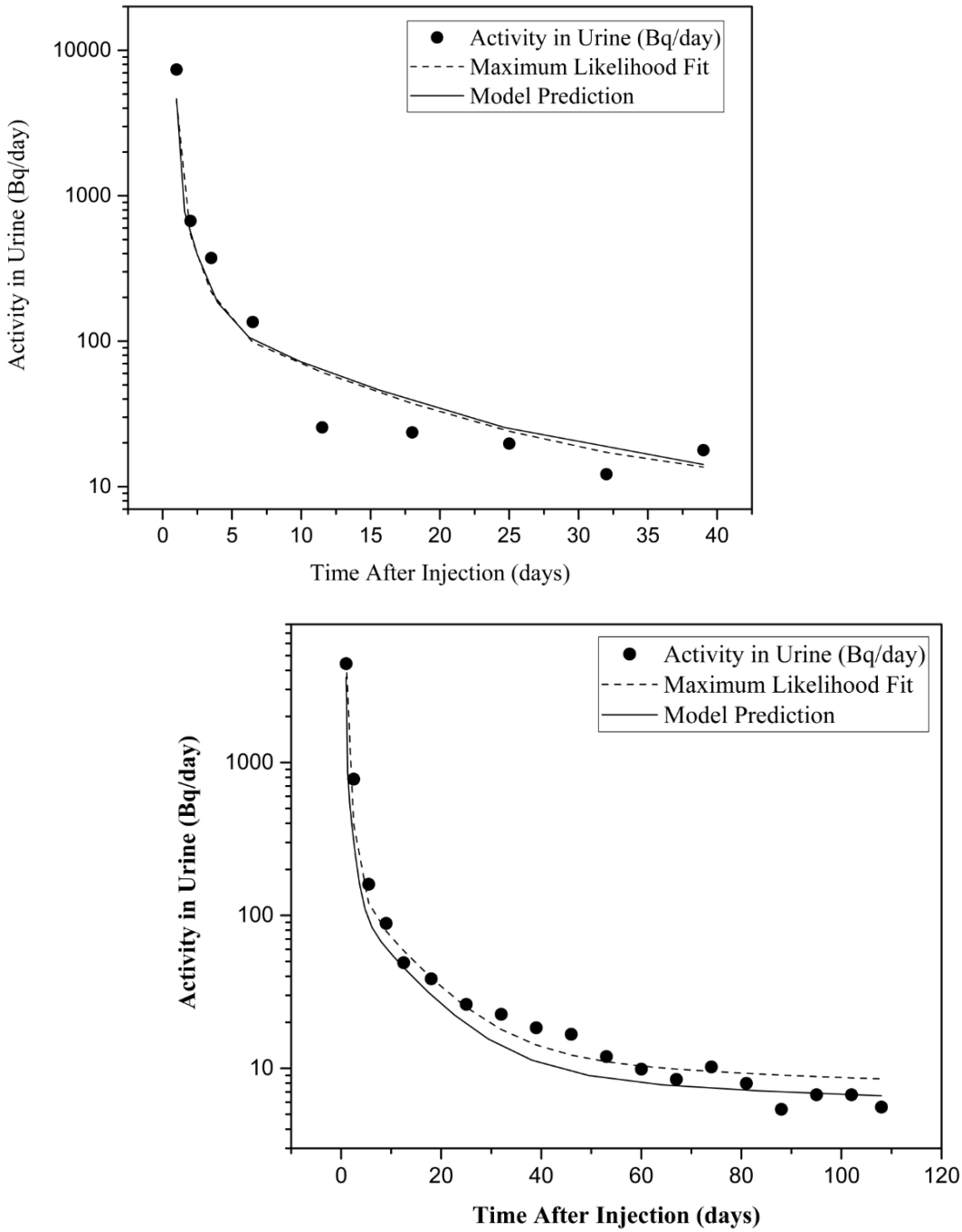

Figure 4.1. Urine prediction for a) C44F and b) C189M using ICRP 67 and NCRP 156 default parameters. The scattered data points correspond with the measured experimental NHP data. The solid line and dash line represents the IMBA prediction of the excretion values of urine as a function of time along with maximum likelihood fit based on the systematic and wound models for ^{241}Am.

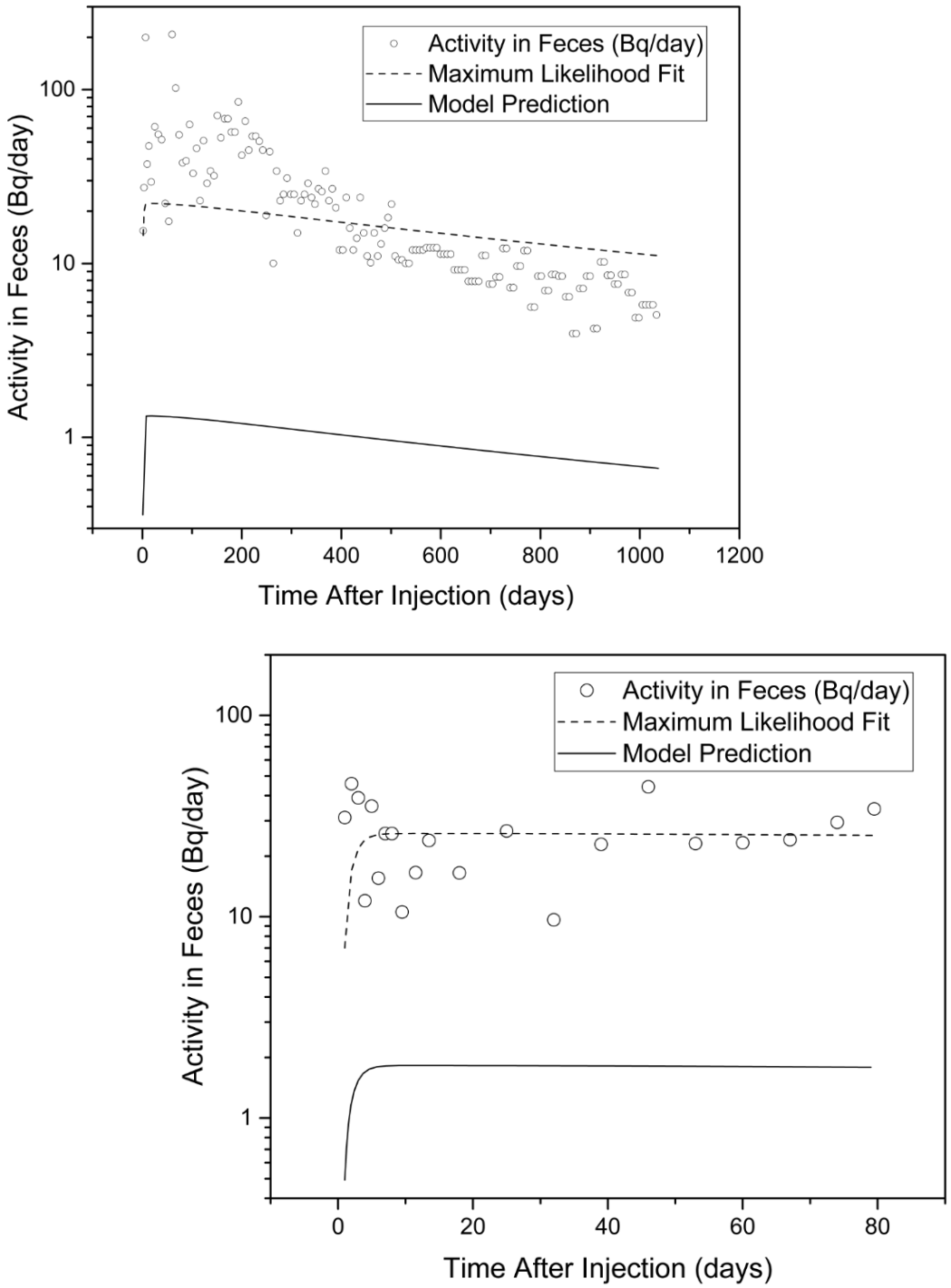

Figure 4.2. Feces prediction for a) C78F and b) C81F using ICRP 67 and NCRP 156 default parameters. The scattered data points correspond with the measured experimental NHP data. The solid line and dash line represents the IMBA prediction of the excretion values of urine as a function of time along with maximum likelihood fit based on the systematic and wound models for ^{241}Am.

To see the results using different patterns, we plotted the activity normalized to animal weight (Bq) vs time (days) using urine data Figure 4.3. The model predictions with the default transfer rates both overestimate and underestimate the experimental intakes. The fact that the model both overestimates and underestimates the intake is a good result, because it shows that predictions are not biased in a specific direction. However, the large range of variation of these results seems to indicate that there are large physiological variabilities between the NHP subjects and humans. From Figure 4.3, it appears that there is more variability among smaller animals regardless of the age of the subject. ICRP 67 is an age depended model and it seems that early predictions are better than late, therefore, there is no correlation between the intake and animal weight.

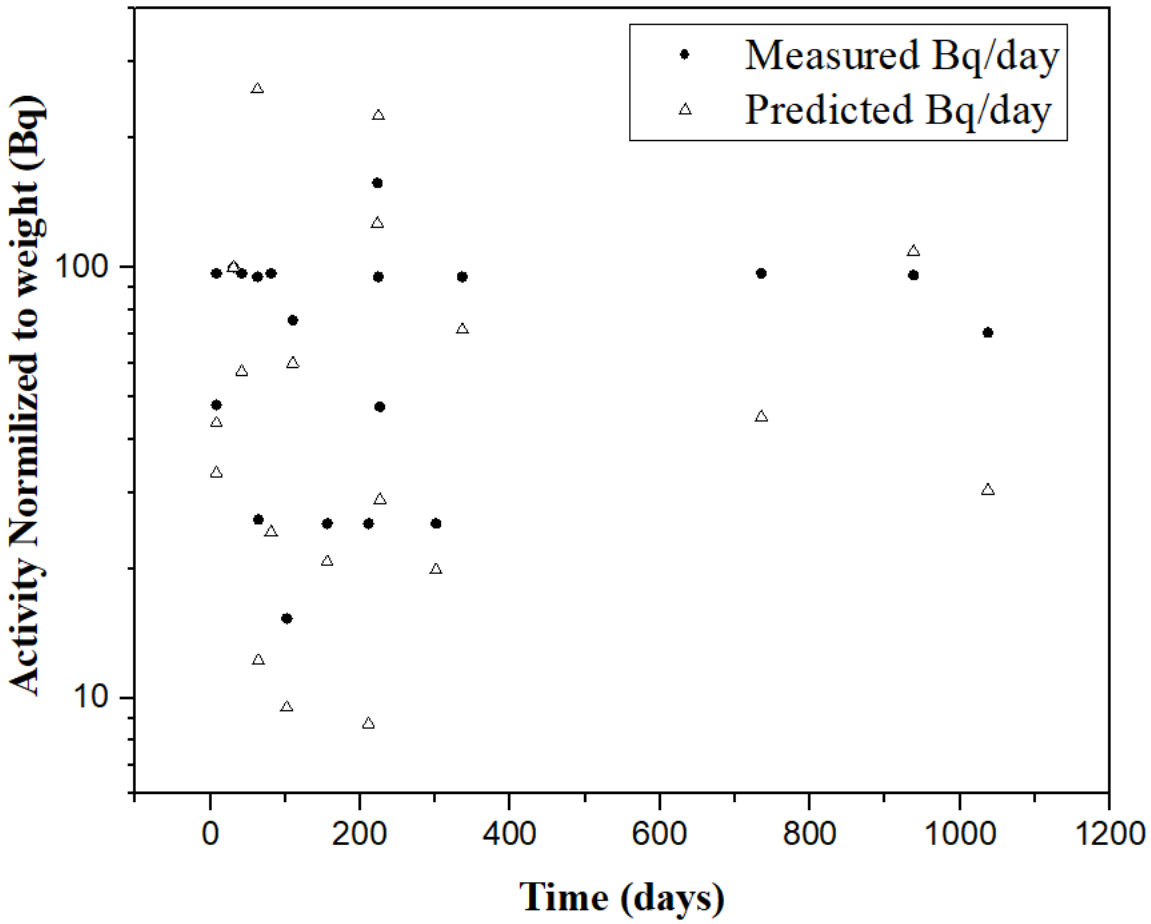

Figure 4.3. The activity normalized to animal weight (Bq) vs time (days) using urine data.

To simplify the comparison and to avoid correcting the data for different intake, six cases injected intramuscularly with 7.47×10^4 Bq of Am citrate were used. The excreta of these animals were averaged from 1 day to 907 days and input into the IMBA software for making better comparison Figure 4.4. It has been demonstrated that the human biokinetic model of ^{241}Am is in agreement with measured data, particularly at the earliest times. After the first week, the model underestimated the actual excretion by values up to 71% the measured values. Predictions of urine excretion up to about 400 days post injection overestimated the measured values by between 2.5 to 268%. However, these same default parameters adequately predicted the injected activity (7.47×10^4Bq). Similar analyses were also done for the feces data for the six cases. Using the ICRP 67 model, the fecal excretion values under-estimated predicted intake by 12.8 time the actual intake.

Americium activity in liver and skeleton at the time of death were calculated using the default transfer rates from the systematic model and wound model. These values were compared to the measured activity at the time of death from Durbin's data. The predictions of the activity retention by default parameters and activity retention in liver and skeleton at the time of death are shown in Table 4.4. In general, the ratio of the predicted activity to measured activity for the liver was more than 1.0 in almost all cases. The most accurate prediction seemed to occur in the cases (C155F, C44F). The ratio tended to be large for animals sacrificed after 40 days post injection ranging from 6.11 to 89 times the actual measured values. The fraction of predicted over measured activity at the time of death in the skeleton was also over 1.0 in most cases and accurate predictions were obtained in 7 cases. The predicted activity in skeleton in all cases ranged from 3 to 13,400% overestimated activity and from 9 to 61% underestimated activity.

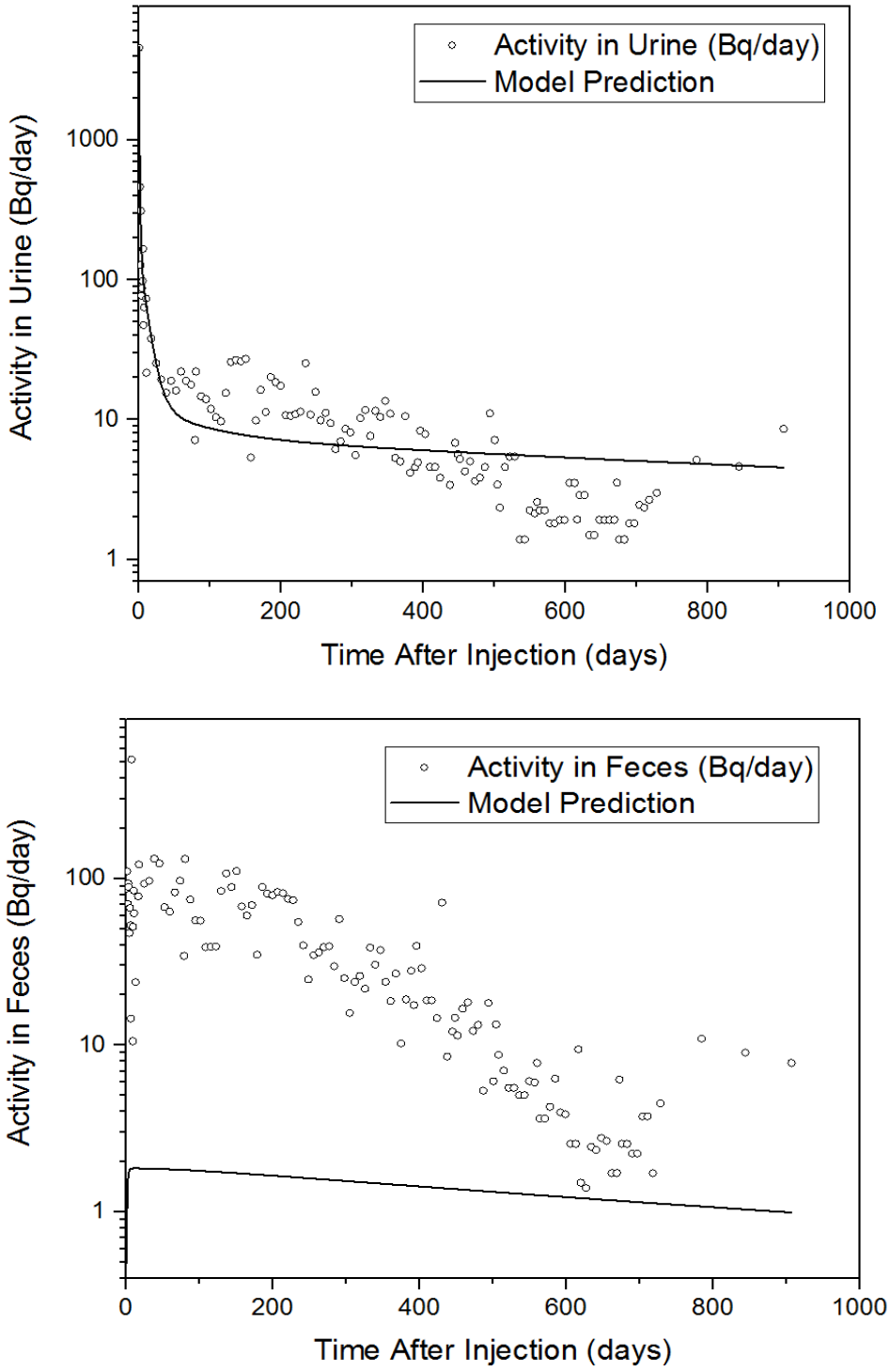

Figure 4.4. Urinary and fecal excretion per day from the NHPs (C138F, C55F, C44F, C81F, C46F, C54F) injected intramuscularly with 7.47×10^4 Bq of Am citrate compared with ICRP 67 reference model. The scattered data points correspond with the measured experimental NHP data. The solid line and dash line represents the IMBA prediction of the excretion values of urine as a function of time along with maximum likelihood fit based on the systematic and wound models for ^{241}Am.

Table 4.4. The fraction of predicted over measured values for liver and skeleton at the time of death

Case[a]	Days from Injection to Death	Liver			skeleton		
		Measured Retention (Bq)	predicted Retention (Bq)	Predicted Retention/ Measured Retention	Measured Retention (Bq)	predicted Retention (Bq)	Predicted Retention/ Measured Retention
C155F	8	21,867	20,781	**0.95**	7,918	12,686	1.60
C138F	8	42,378	86,629	2.04	18,834	52,882	2.81
C55F	21	28,568	43,261	1.51	29,894	27,040	**0.90**
C6F	31	36,710	62,039	1.69	292.448	39,471	134.97
C44F	42	35,427	35,520	**1.00**	22,048	23,035	**1.04**
C56F	63	26,007	159,000	6.11	22051.26	106,800	4.84
C146M	64	10,549	7,506	0.71	4,915	5,050	**1.03**
C81F	81	28,326	14,805	0.52	26,682	10,239	0.38
C162F	102	1,729	5,714	3.31	3,943	4,084	**1.04**
R189M	110	3961.738	35,879	9.06	30,323	25,962	**0.86**
C157F	156	2,079	9,114	4.38	5981.05	7,040	**1.18**
C158F	211	5,967	8,762	1.47	6,573	7,333	**1.12**
R118M	223	21,052	53,613	2.55	45,607	59,651	1.31
C57F	224	1,399	124,560	89.02	32,601	106,100	3.25
C110F	226	2,418	16,181	6.69	21,941	13,820	0.63
C156F	301	2078.66	8,190	3.94	5,981	7,710	1.29
C45F	336	1120.878	36,464	32.53	27,326	35,847	1.31
C46F	735	1,487	22,735	15.29	24,440	34092	1.39
C54F	938	667	19637	29.42	26,270	35170	1.34
C78F	1037	4,960	13540	2.73	19,037	26,258	1.38

[a]M= male, F= female.

4.2. Comparing the Results of Nonhuman Primates with Other Animals from Previous Studies

Table 4.5 contains the percentage of injected activity excreted in urine and feces weekly and monthly for NHP injected with 7.47×10^4 Bq of Am citrate. The results of the NHP excreta analyses were compared to the results from previous studies on beagle dogs and baboons. Six percent of the injected activity was excreted in urine and approximately 0.1% in feces in the first 24h. Between the first week and 2nd month, about 8.6% of Am excretion was excreted in urine. Fecal excretion represents less than 1% of total in the first week and nearly 3% of the calculated excreted activity by the end of the first 2 months. Hence, it is observed that until the end of 907 days post injection, the excretion of ^{241}Am in these animals was predominantly urinary and most of the cumulative americium excretion was urinary; however, the fecal to urinary clearance ratio varied from 0.11 during the first week to 9.89 at the end of 8 months with the fecal route becoming to dominated by the end of 3rd week. The results from NHP did differ from excreta analysis in other species such as beagle dogs and baboons. Urinary excretion in the beagle is the dominate pathway of clearance with no evidence that the feces excretion route will ever become clearance the dominant pathway (Lloyd et al. 1970). In contrast, fecal excretion in the baboons is considered the major pathway by the end of the second week (Rosen et al. 1972, Guilmette et al. 1980).

Measured liver and skeleton retention at the time of death were compared to those for beagle dogs and baboons. The curves in Figure 4.5 shows an initial retention in NHP of about 55% liver and 25% skeleton for animals injected with ^{241}Am, comparing to 43% liver and 47% skeleton retention in the beagle but 30% liver retention in the baboon. The results of the tissue distribution of Durbin NHP subjects at the time of sacrifice showed approximately 1% and 35% of the retained materials was accounted for the liver and skeleton deposition, respectively. This can be contrasted to the experience with the beagle data in which 25% liver and 48% skeleton retention is observed.

A likewise comparison shows baboons with 2% liver retention. NHPs data showed that the fraction of the injected activity found in the liver was greater immediately following injection. After 42 days, the activity deposition in the liver typically decreased to about 47%, and this was followed by a sharp decrease thereafter. Skeleton ^{241}Am retention started to increase after 700 days. The skeleton burden trended to increase until the death of the animals.

For Durbin monkeys, the rate of elimination of americium from the liver is more rapid (81-days) than in beagle (154 days), however, the rate is slower than in baboon where 88% of the liver content was cleared within (28 day). As it appears in Figure 4.4, after 100 days, the ^{241}Am begins leaving the liver and at least part of the activity is redeposited in the skeleton.

Table 4.5. Excreta analysis for cases injected intramuscularly with 7.47×10^4 Bq of Am citrate

	% of injected activity excreted				
Time	**Urine**	**Feces**	**Total (U and F)**	**Cumulative Total**	**Ratio F/U**
1st W[a]	7.96	0.84	8.81	8.81	0.11
3rd W	0.48	1.27	1.75	10.56	2.64
1st M[b]	0.06	0.25	0.31	10.87	4.25
2nd M	0.10	0.43	0.53	11.40	4.43
3rd M	0.09	0.55	0.64	12.04	6.20
4th M	0.07	0.30	0.37	12.41	4.42
5th M	0.10	0.36	0.46	12.87	3.46
6th M	0.09	0.44	0.53	13.40	4.77
7th M	0.11	0.37	0.48	13.88	3.28
8th M	0.04	0.43	0.47	14.35	9.89
9th M	0.08	0.26	0.34	14.70	3.05
10th M	0.05	0.20	0.25	14.95	4.06
11th M	0.06	0.17	0.23	15.17	3.10
12th M	0.04	0.15	0.19	15.36	3.56
13th M	0.05	0.15	0.20	15.56	2.72
14th M	0.04	0.14	0.17	15.74	3.46
15th M	0.03	0.14	0.18	15.91	4.15
16th M	0.03	0.16	0.19	16.10	6.14
17th M	0.02	0.08	0.10	16.20	3.21
18th M	0.04	0.07	0.12	16.32	1.86
19th M	0.02	0.04	0.06	16.38	1.51
20th M	0.01	0.04	0.05	16.43	3.08
21st M	0.01	0.02	0.03	16.47	2.20
22nd M	0.02	0.03	0.05	16.51	1.74
23rd M	0.01	0.01	0.02	16.54	0.88
24th M	0.02	0.02	0.04	16.57	1.34
25th M	0.01	0.01	0.02	16.59	1.50
26th M	0.01	0.02	0.03	16.62	1.30
27th M	0.01	0.01	0.02	16.65	2.12
28th M	0.01	0.01	0.02	16.66	1.95
29th M	0.01	0.01	0.02	16.69	0.91

[a]W= Week.
[b]M= Month.

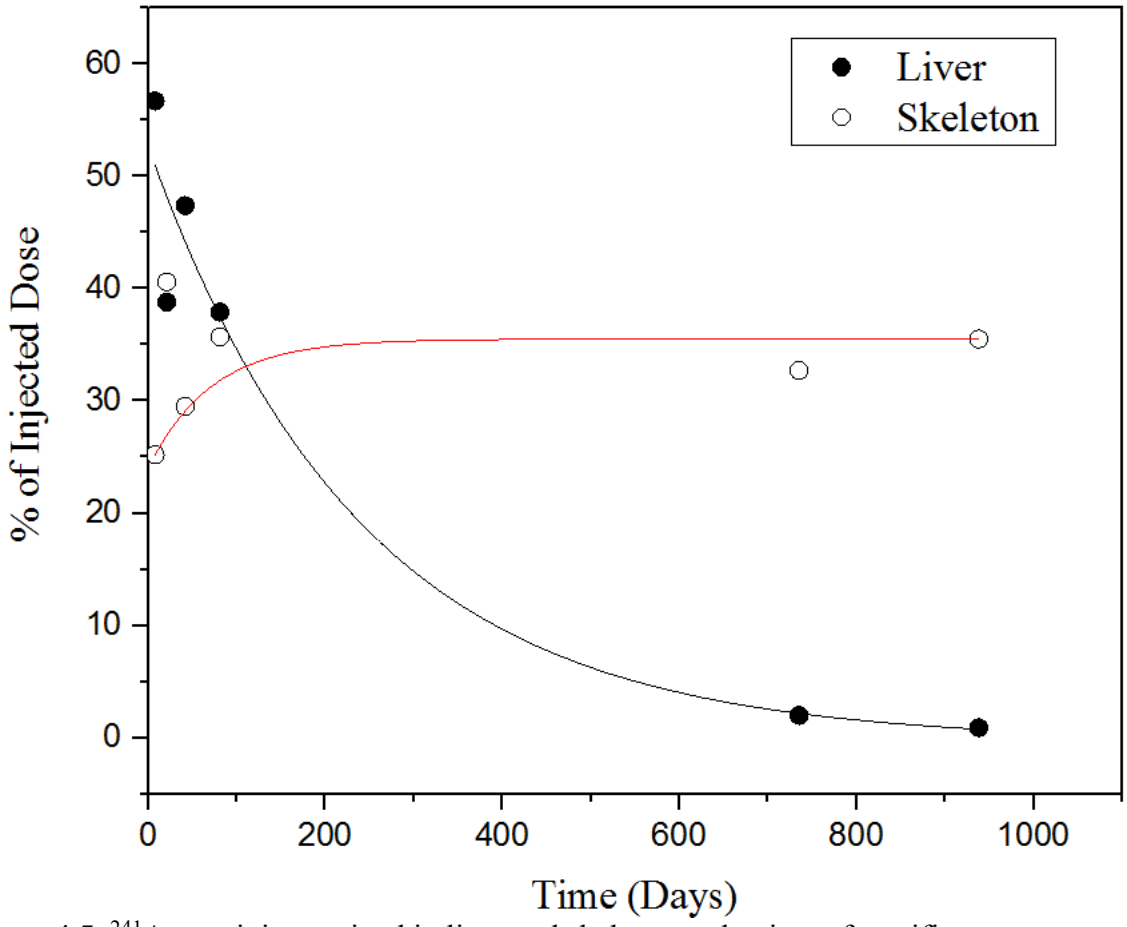

Figure 4.5. ^{241}Am activity retained in liver and skeleton at the time of sacrifice

Table 4.6 provides other bone, organs, and tissues retention of the same six NHP used in investigation to show the whole picture of americium deposition in addition to the liver and skeleton. Noticeably, the liver and skeleton are the main organs of Am deposition, while, the other organs or tissues have only a minor amount of retained activity. Less than 1% of injected ^{241}Am was retained in the kidneys, spleen, teeth, and tail in comparison to the 1 to 2% that was observed in muscles, pelt, and kidneys of beagle dogs. It appears that in NHP experiences, muscles contain a relatively large amount of activity retained activity (3%) and perhaps should be consider an important tissue in addition to the liver and skeleton. In general, soft tissues and organs other than

liver, skeleton, and muscles are not seemingly important in the NHP that were investigated by Durbin due to the low percentage of activity deposition in these tissues and organs.

Table 4.6. Distribution of ^{241}Am in NHP soft tissues. Numbers in parentheses next to the animals identification codes are the days between injection and sacrifice.

	% of injected dose					
Organ or tissue	**C138F (8d[a])**	**C55F (21d)**	**C44F (42d)**	**C81F (81d)**	**C46F (735d)**	**C54F (938d)**
Liver	56.70	38.80	47.40	37.90	1.99	0.90
Kidneys	0.72	0.50	0.13	0.27	0.01	0.05
Spleen	0.12	0.06	0.06	0.13	0.01	0.02
Muscle	3.16	2.70	1.41	1.36	0.54	0.91
Pelt	NM	1.64	NM[b]	NM	0.25	0.68
Bones	25.20	40.60	29.50	35.70	32.70	35.50
Teeth	0.26	0.60	0.56	0.40	0.53	0.70
Tail	0.38	0.27	1.83	2.02	2.17	1.24

[a]d= days
[b]NM= Not Measured.

The ICRP 67 biokinetic model for Americium describes the long-term activity elimination and retention of this Am in the human body. The current effort compared the prediction of the ICRP 67 americium model with measured NHP data obtained from short-term experiments from 8 to 907 days post intake. Thus, the comparison between NHP and human is difficult. The difficulties in predicting the intake and organ retention can be explained by the physiological differences between the NHP and human, as well as the differences in the amount of activities translocated or deposited in the liver tissue and non-liver tissues (primary skeleton). The processes that control uptake, retention, and clearance of americium by the liver depend on the amount of administrated activity. Within hours after administration, americium is distributed uniformly in the portion of the liver which contains the parenchymal cells. There are two mechanisms of elimination of retained activity from liver to skeleton depending on the level of injected activity (Leggett 1992). Radiation-induced death mechanism was explained by Lloyd et al. (1970) for high

level activity (about 2.8 μCi/kg) where the reduction of the activity in the liver is due to the radiation damage to the liver. Americium is tightly bound in the liver and after the tissue is damaged, the liver starts to release its activity that is eventually deposit in the skeleton. The rate of activity transfer to skeleton according to Lloyd et al. depends on the time needed to deliver sufficient radiation dose to destroy the liver cells directly or damage them during cellular division. This is thought to be a very species dependent effect (Lloyd et al. 1070). Biliary secretion rate in the liver consider another mechanism for transferring americium from liver to non-liver tissues. The biliary secretion rate in monkeys is very rapid compared to that in beagles or human (Lloyd et al. 1997). Therefore, the Am in the liver is eliminated and transferred to the skeleton after a shorter period of time. The absolute life span of humans and NHP is much different. We anticipate that relative translocation will occur more rapidly in the NHP. This may be the reason that the liver retention in NHP is over-estimated after 40 days post injection when using the human model. The overestimation in liver retention tends to be consistent with the over-estimation in fecal excretion in the NHP. Fecal excretion of americium is assumed to arise from the biliary secretion from the liver into the GI tract content via secretion in hepatic bile. In addition, during skeleton remodeling, most of the activity tends to be removed from the bone surface and transferred to feces excreta (Lloyd et al. 1997). Therefore, the fecal excretion should be increased when considering NHP.

4.3.Modification of ICRP 67 and NCRP 156 Default Transfer Rates.

Based on the previous work, it appears that suggested ICRP 67 and NCRP 156 models did not adequately predict the ^{241}Am intake and skeleton retention in NHPs. Therefore, develop alternative values for wound and systemic model transfer rates were necessary in the effort to improve biokinetic prediction of ^{241}Am based on bioassay and autopsy data of NHPs injected intramuscularly with $^{241}Am(NO_3)_3$.

After carefully review the predictions based on the default parameters as reproduced in Table 4.2, NHPs were divided into two groups depending on the time between injection and sacrifice (early and late sacrificed animals). It has been demonstrated that the human models of the biokinetics of ^{241}Am are in agreement with measured data, particularly at the earliest times (less than 100 days) such as in C44F and C55F (Figure 4.6 a,b) and Table 4.7. However, the models were unable to describe the excretion rates 100 days post intake as well as the activities in the skeleton at autopsy. The NHP cases providing data from more than 100 days post intake were divided into two subgroups based on the level of the intake experienced by each animal. These were categorized as intermediate and high intake. Intermediate levels of intake ranged from 1.96×10^4 to 5.44×10^4 Bq and high levels of intake ranged from 7.3×10^4 to 12×10^4 Bq.

To optimize the default transfer rate parameters, IMBA-UA loaded the customized wound and systemic transfer rate parameters from the IMBA Professional Plus software. The most sensitive parameters were selected to be sampled. A log-uniform distribution was selected for each parameter modeled as a *prior* distribution. Parameters were limited, based on an assumption, to a range from 1/10 to 10 times the human parameters. A Latin hypercube method was used as a random sampling methods to form n×N sample matrix, where (N) is the specified number of iterations ($N=10^3$) and (n) is the number of biokinetic parameters that were varied (Puncher and Birchall 2008). Parameters with the lowest χ^2-value were considered the values that best predicted the NHPs intake and activity in the skeleton at the time of death. Predictions based on the new transfer rate values were then compared to the predictions made using the default parameters.

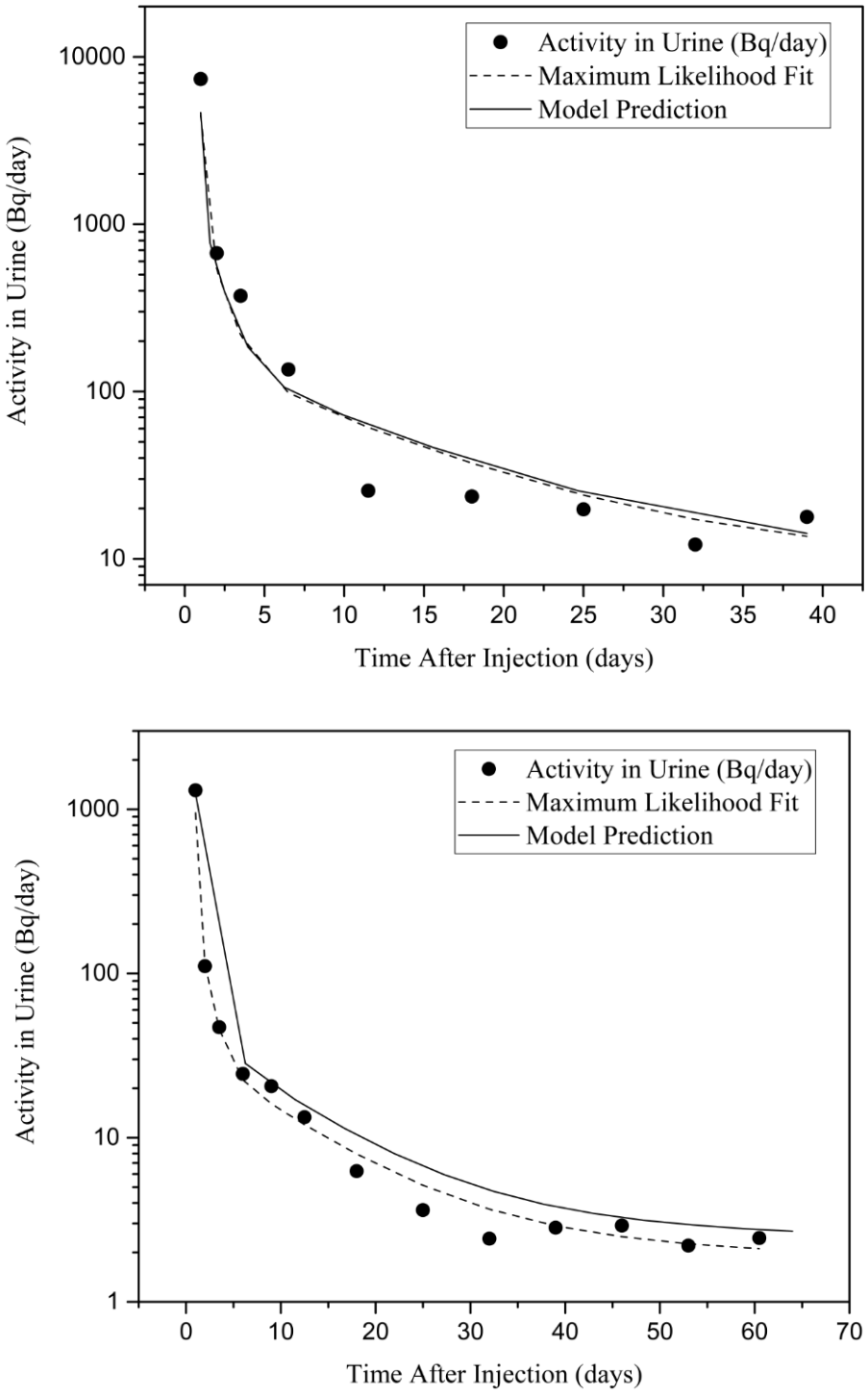

Figure 4.6. Urine prediction for a) C44F and b) C55F using ICRP 67 and NCRP 156 default parameters. The scattered data points correspond with the measured experimental NHP data. The solid line and dash line represents the IMBA prediction of the excretion values of urine as a function of time along with maximum likelihood fit based on the systematic and wound models for ^{241}Am.

Table 4.7. Case C138 and C44F using ICRP68 and NCRP156 default parameters

Case #		ICRP 67 model
C55F	Error in intake prediction	18%
	Total chi-square	1.07
	(p value)	0.99
	Error in prediction of activity in skeleton	-23%
C44F	Error in intake prediction	-4%
	Total chi-square	6.79
	(p value)	0.56
	Error in prediction of activity in skeleton	9%

Prior to the optimization analysis, one case from the intermediate intake cohort (more than 100 days) and two cases from high intake cohort (from 63 to 300 days) and (above 300 days) were selected randomly (R189M, C56F and C78F) so that they could later be used to validate and test the developed model. The combined wound and systemic model contains 29 different inter compartmental transfer rates. The most sensitive parameters selected to be optimized for the NHP population along with the new parameters are shown in boldface in Table 4.8. To verify how well the developed model described in Table 4.8 predicted the known intake and the retention values in skeleton, the model was tested with the selected animal cases using the maximum likelihood analysis and the chi-square values with the lowest associated p values.

The sensitive parameters proved to be helpful in identifying the pathways and hypothetical physiological processes associated with the model compartments that most influenced the predictions of intake and organ burden. The parameter associated with the intermediate soft tissues compartment (ST1) that exchanged material to blood proved to be the most influential pathways in the model for the two periods and was selected to be optimized. The parameter associated with the fast soft tissues compartment (ST0) was considered the most important only for cases with high intakes and which lived less than 300 day. At less than 300

days, the parameters associated with bone resorption such as the trabecular bone surface was also very influential, while transfer from trabecular bone volume to marrow were selected to be optimized for cases that lived more than 300 days after they were injected with high dosage. The parameters associated with urinary excretion including the exchange of the activity between the kidney and blood were chosen to be optimized to account for the differences in urine excretion rates in humans and NHPs for animals that were injected with a high level of activity. Moreover, the exchange of activity between the liver and the blood was optimized to account for the differences in the activity residing in the liver for only the cases injected with high intakes that lived more than 300 days.

Table 4.8. The modified transfer rates that explained the biokinetics of ^{241}Am in each group of NHPs

Transfer Rate (d^{-1})								
Route of Transfer Rate Between Compartments		ICRP 67	Optimized model					
Source	**Target**		**Intermediate Intake (100-300 d)**	**Differences**	**High Intake (63-300 d)**	**Differences**	**High Intake (300 d)**	**Differences**
Blood	Liver	1.16×10^{1}	1.16×10^{1}	0.00	1.16×10^{1}	0.00	1.16×10^{1}	0.00
Blood	CS[a]	3.49	3.49	0.00	3.49	0.00	3.49	0.00
Blood	TS[b]	3.49	3.49	0.00	3.49	0.00	3.49	0.00
Blood	UBC[c]	1.63	1.63	0.00	1.63	0.00	1.63	0.00
Blood	Kidneys (Upath[d])	4.66×10^{-1}	4.66×10^{-1}	0.00	4.66×10^{-1}	0.00	4.66×10^{-1}	0.00
Blood	OKT[e]	1.16×10^{-1}	1.16×10^{-1}	0.00	1.16×10^{-1}	0.00	**1.71×10^{1}**	**146**
Blood	ULI[f]	3.03×10^{-1}	3.03×10^{-1}	0.00	3.03×10^{-1}	0.00	3.03×10^{-1}	0.00
Blood	Testes	8.20×10^{-3}	8.20×10^{-3}	0.00	8.20×10^{-3}	0.00	8.20×10^{-3}	0.00
Blood	Ovaries	2.60×10^{-3}	2.60×10^{-3}	0.00	2.60×10^{-3}	0.00	2.60×10^{-3}	0.00
Blood	ST0[g]	1.00×10^{1}	1.00×10^{1}	0.00	1.00×10^{1}	0.00	1.00×10^{1}	0.00
Blood	ST1	1.67	1.67	0.00	1.67	0.00	1.67	0.00
Blood	ST2	4.66×10^{-1}	4.66×10^{-1}	0.00	4.66×10^{-1}	0.00	4.66×10^{-1}	0.00
ST0	Blood	1.39	1.39	0.00	**3.18×10^{-2}**	**43.00**	1.39	0.00
ST1	Blood	1.39×10^{-2}	**3.75×10^{-1}**	**26**	1.39×10^{-2}	0.00	**2.59×10^{1}**	**1862**
ST2	Blood	1.90×10^{-5}	1.90×10^{-5}	0.00	1.90×10^{-5}	0.00	1.90×10^{-5}	0.00
CV[h]	CM[i]	8.21×10^{-5}	8.21×10^{-5}	0.00	8.21×10^{-5}	0.00	8.21×10^{-5}	0.00
CS	CV	4.11×10^{-5}	4.11×10^{-5}	0.00	4.11×10^{-5}	0.00	4.11×10^{-5}	0.00

Transfer Rate (d^{-1})								
Route of Transfer Rate Between Compartments		**ICRP 67**	**Optimized model**					
Source	**Target**		**Intermediate Intake (100-300 d)**	**Differences**	**High Intake (63-300 d)**	**Differences**	**High Intake (300 d)**	**Differences**
CS	CM	8.21×10^{-5}	8.21×10^{-5}	0.00	8.21×10^{-5}	0.00	8.21×10^{-5}	0.00
TV[j]	TM[k]	4.93×10^{-4}	4.93×10^{-4}	0.00	4.93×10^{-4}	0.00	**1.97×10^{-2}**	**39.0**
TS	TV	2.47×10^{-4}	2.47×10^{-4}	0.00	2.47×10^{-4}	0.00	2.47×10^{-4}	0.00
TS	TM	4.93×10^{-4}	**3.39×10^{1}**	**68762**	4.93×10^{-4}	0.00	4.93×10^{-4}	0.00
TM	Blood	7.60×10^{-3}	7.60×10^{-3}	0.00	7.60×10^{-3}	0.00	7.60×10^{-3}	0.00
CM	Blood	7.60×10^{-3}	7.60×10^{-3}	0.00	7.60×10^{-3}	0.00	7.60×10^{-3}	0.00
Live	Blood	1.85×10^{-3}	1.85×10^{-3}	0.00	1.85×10^{-3}	0.00	**7.91×10^{-1}**	**427**
Liver	GI Tract	4.90×10^{-5}	4.90×10^{-5}	0.00	4.90×10^{-5}	0.00	4.90×10^{-5}	0.00
Testes	Blood	1.90×10^{-4}	1.90×10^{-4}	0.00	1.90×10^{-4}	0.00	1.90×10^{-4}	0.00
Ovaries	Blood	1.90×10^{-4}	1.90×10^{-4}	0.00	1.90×10^{-4}	0.00	1.90×10^{-4}	0.00
OKT	Blood	1.39×10^{-3}	1.39×10^{-3}	0.00	**2.48×10^{-2}**	**17**	1.39×10^{-3}	0.00
Kidneys (Upath)	UBC	9.90×10^{-2}	9.90×10^{-2}	0.00	9.90×10^{-2}	0.00	9.90×10^{-2}	0.00

[a] CS- Cortical Surface, [b] TS- Trabecular Surface, [c] UBC- Urinary Bladder Content, [d] Upath- Urinary Path, [e] OKT- Kidneys (Other Tissue), [f] ULI- Upper Large Intestine, [g] ST- Soft tissue, [h] Cortical Volume, [i] CM- Cortical Marrow, [j] TV- Trabecular Volume, [k] TM- Trabecular Marrow.

[l]Difference= $\frac{optimized\ parameter - human\ refrence\ parameter}{human\ refrence\ parameter}$

4.4.Optimized Model Parameters Verification.

Optimized parameters for each group of animals were input into IMBA to generate biokinetic predictions for urine along with maximum likelihood fit parameters for each set of measured bioassay data. The results of only three cases (R189M, C56F, and C78F) are plotted and reported in Figures (4.7,4.8,4.9) and Table 4.9 to illustrate the trends observed in all cases. In general, the urine predictions made, that were based on the optimized model were better than the predictions made based on the default human model. These also were improved for predictions of the intake and skeleton retention at different times post intake. The optimized predictions are compared with model predictions in the same figures and table. The difference between the measured values and the maximum likelihood line is improved, these observations indicate the goodness of fit, as well as the difference between the predicted and actual intake, represented by the difference between the maximum likelihood line and the prediction line, was improved and the discrepancy between the two lines is reduced using the modified model.

The optimized parameters were an improvement for all three cases. The prediction of intake and skeleton burden were better than using the default model. The chi-square parameter was reduced compared to that obtained using default parameters for case C56F. However, the intake was still overpredicted by 218% using the optimized model compared to the 342% overprediction using default model for case C56F. The optimized parameters did not, however, improve the fit in case C78F. In case C78F an increase in χ^2 values for urine was observed, although, the new model did marginally improve the prediction of the intake and skeleton burden compare to predictions made based on the human model default parameters.

Table 4.9. Verification of the NHP model using test cases

Case #		ICRP 67 model	Optimized Model
R189M	Error in intake prediction[a]	28%	-0.4%
(Intermediate Intake)	Total chi-square	5.15	8.44
(100- 300 d)	(p value)	1.00	0.971
	Error in prediction of activity in skeleton[b]	-14%	3%
C56F	Error in intake prediction	342%	218%
(High Intake)	Total chi-square	32.40	10.9
(63-300 d)	(p value)	0.00	0.456
	Error in prediction of activity in skeleton	384%	-0.3%
C78F	Error in intake prediction	-30%	-15%
(High Intake)	Total chi-square	149	198
(above 300 d)	(p value)	0.536	0.00
	Error in prediction of activity in skeleton	38%	7%

[a] The differences between the known intake and the intake estimated

[b]The difference between the known activity in skeleton and the activity predicted by the model in the skeleton.

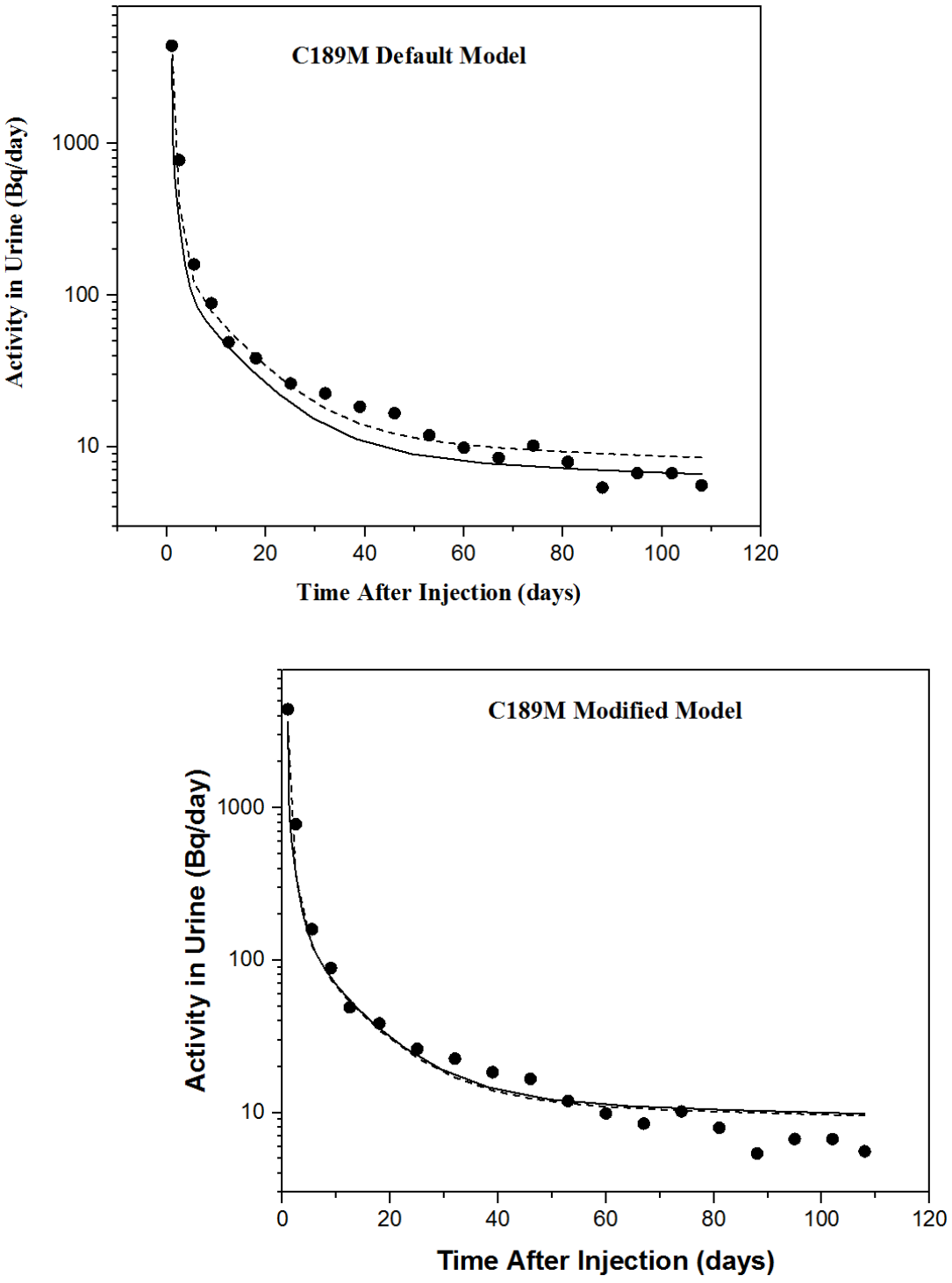

Figure 4.7. Model predicted and fitted activity of urine data using default and modified parameters for R189F. The scattered data points correspond with the measured experimental NHP data. The solid line and dash line represents the IMBA prediction of the excretion values of urine as a function of time along with maximum likelihood fit based on the systematic and wound models for ^{241}Am.

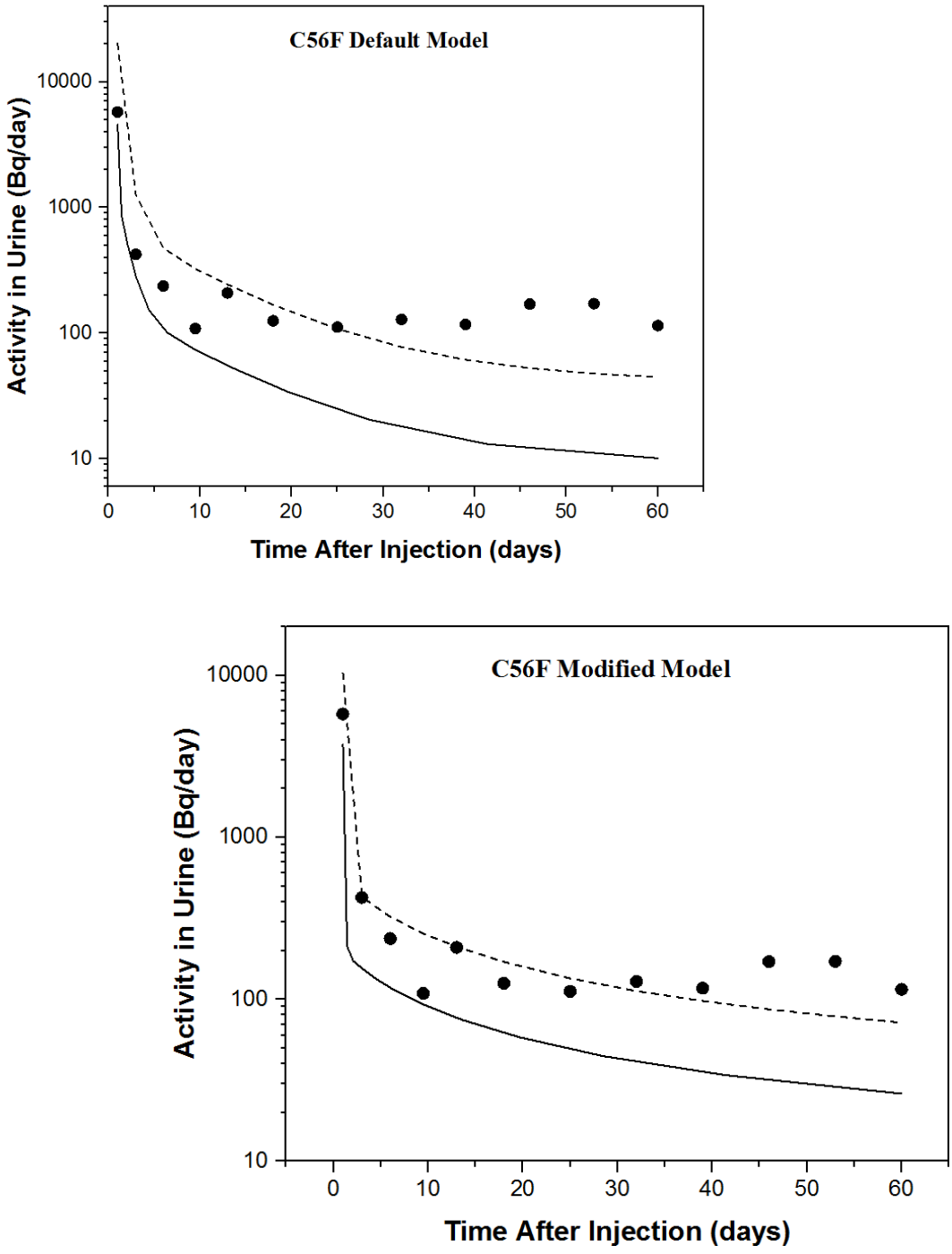

Figure 4.8. Model predicted and fitted activity of urine data using default and modified parameters for C56F. The scattered data points correspond with the measured experimental NHP data. The solid line and dash line represents the IMBA prediction of the excretion values of urine as a function of time along with maximum likelihood fit based on the systematic and wound models for ^{241}Am.

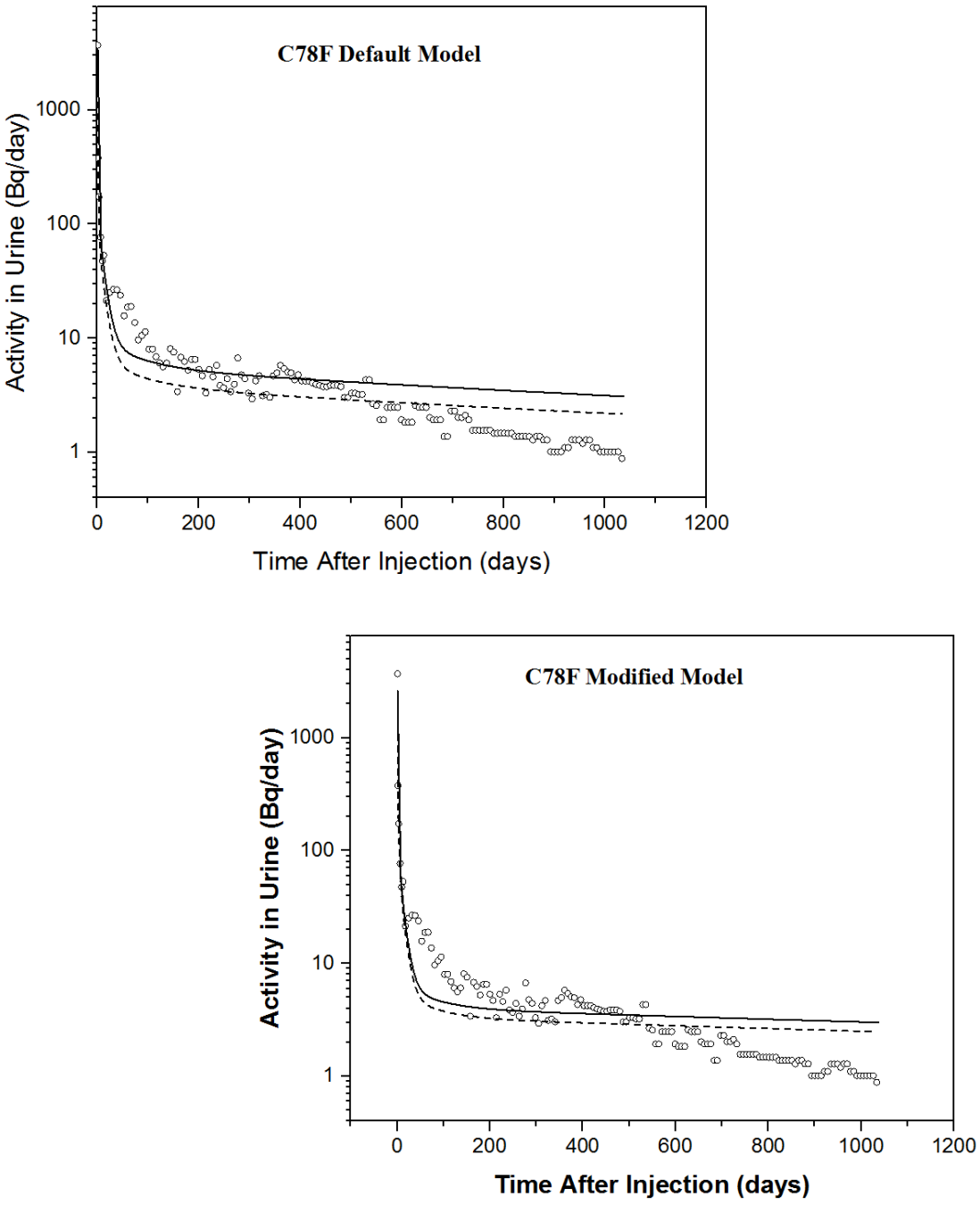

Figure 4.9. Model predicted and fitted activity of urine data using default and modified parameters for C78F. The scattered data points correspond with the measured experimental NHP data. The solid line and dash line represents the IMBA prediction of the excretion values of urine as a function of time along with maximum likelihood fit based on the systematic and wound models for ^{241}Am.

The remaining cases were also tested using the optimized model parameters and these predictions were compared with those obtained using ICRP/NCRP default transfer rates. The histograms in Figures 4.10 and 4.11 show the differences of the relative error of predicted intake and the activity retained in skeleton using the default and optimized wound and systemic model parameters. The intakes were predicted well using the optimized parameters in 66% of the cases used in this validation. The prediction of the intake ranged from 218% overprediction to 66% underprediction for the remaining 34% cases. The activity predicted to be retained in the skeleton improved in almost all cases where the differences between the predicted and measured activity is a value less than 20%. The effect of using the optimized parameters were unclear in 3 cases since the fit was not substantially improved. The model fit was worsened in cases C45F, C46F, and C78F using the optimized parameters with lower χ^2.

Although most pathways between humans and monkeys are similar, there are differences between humans and these NHP with respect to liver and skeleton metabolism. The changes made in the parameters selected were useful to explain the overestimation of the intake and skeleton retention in monkeys demonstrating that the act of increasing the rate of elimination of activity from liver to blood and from trabecular bone to trabecular marrow compartments was an action in the correct direction when modeling NHP. The validation of the suggested transfer rates shows that the intake and skeleton retention were predicted better than using default model parameters but somewhat this enhancement is marginal because the modified parameters did not improve the fit where the values of the χ^2 were less than 0.05.

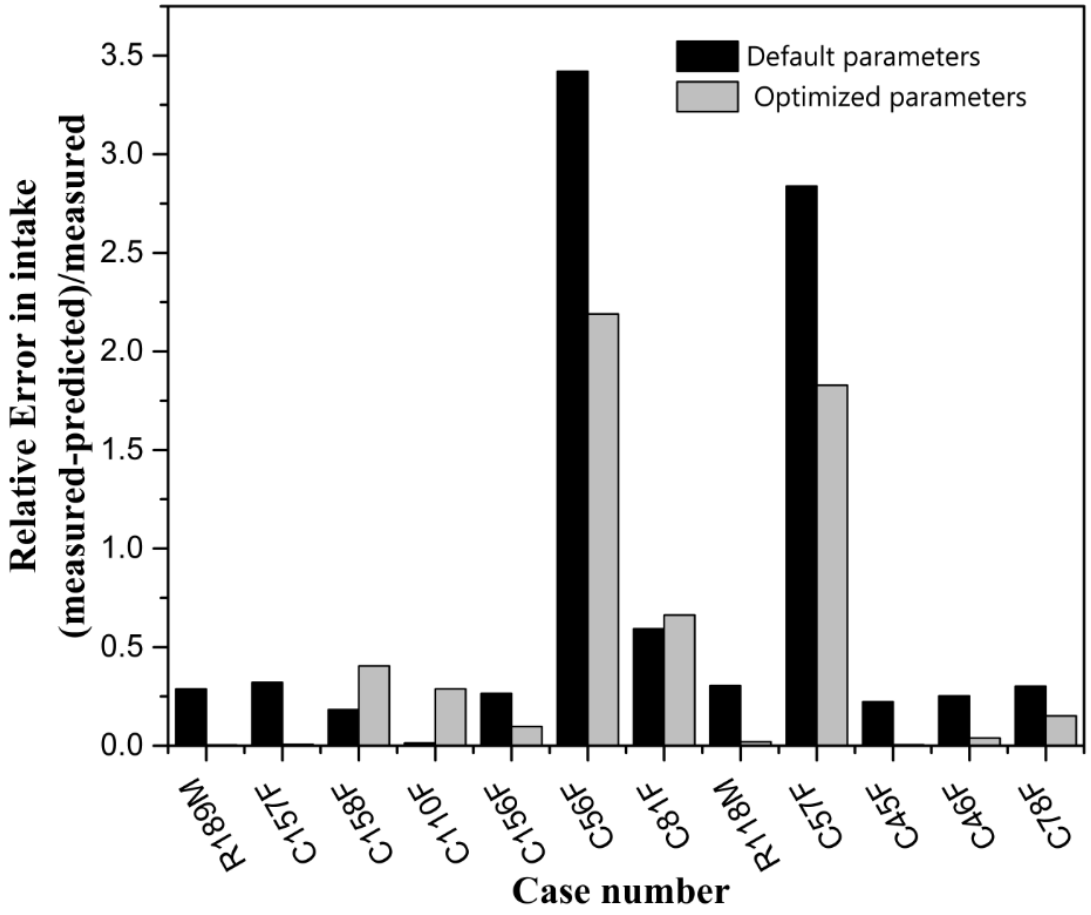

Figure 4.10. A comparison of the relative error in intake using the default or optimized parameters.

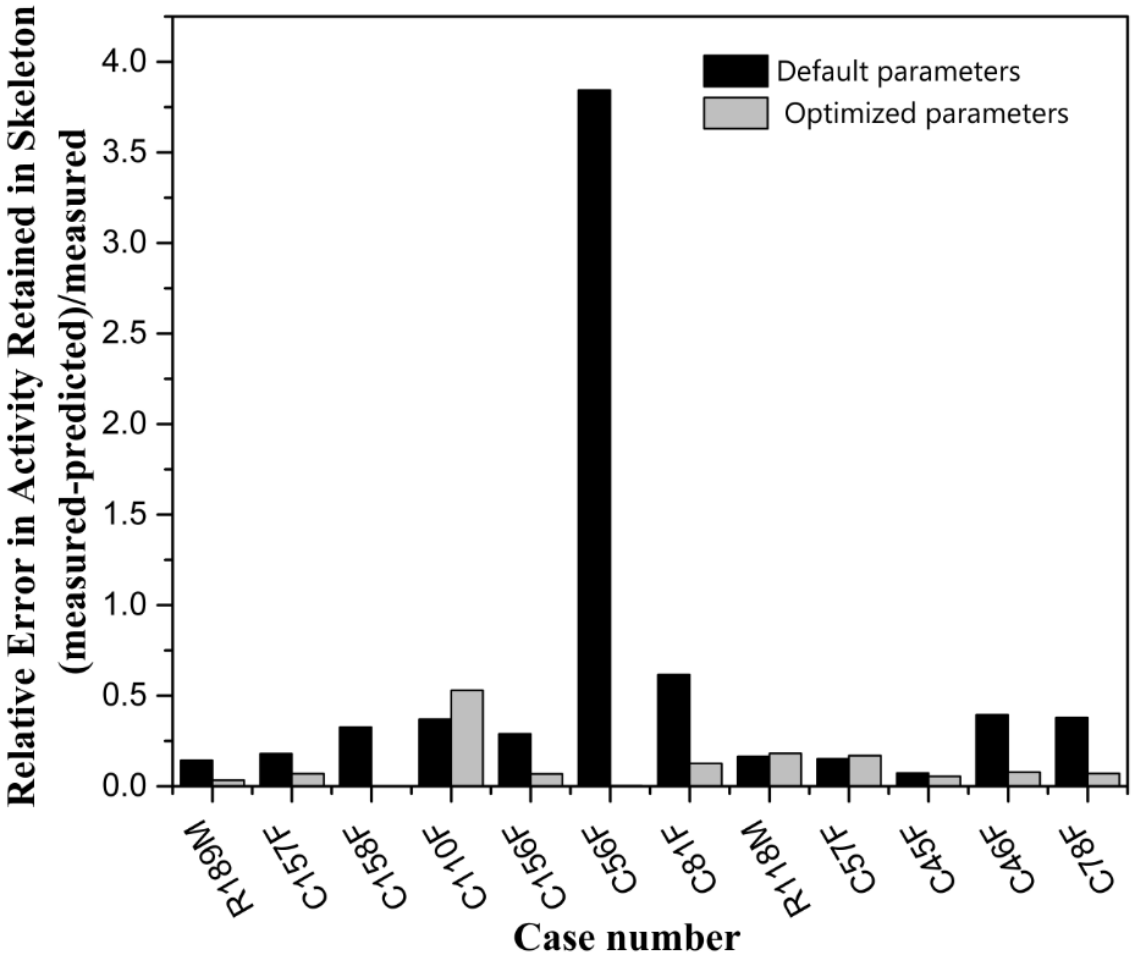

Figure 4.11. A comparison of the relative error in activity retained in skeleton using the default or optimized parameters

Chapter 5:

Conclusion.

ICRP67/NCRP156 human models and default transfer parameters predicted the intake and the activity residing in the skeleton (typically for less than 100 days post intake). However, the predictions were questionable for animals that lived longer. Typically, when considering longer lived animals, the activity retained was overestimated in almost all cases. Urinary excretion in the monkeys and beagle is the dominate pathway of clearance, in contrast, fecal excretion in the baboons is considered the major pathway by the end of the second week. An initial retention in NHP of about 55% liver and 25% skeleton for animals injected with ^{241}Am, can be compared to 43% liver and 47% skeleton retention in the beagle but 30% liver retention in the baboon. The effort of this project was to develop new transfer rate values that best estimate the injected activity and skeleton retention post intake. When the most sensitive default parameters were altered and the altered values used to enhance predictions, the predictions of intake and skeleton activity were improved for most cases. Therefore, it is suggested that the optimized model could be used to predict the intake and skeleton retention for nonhuman primates better than ICRP 78 and NCRP 156 in the long term.

Chapter 6:

Future works.

In the immediate future, the validity of ICRP 67 and NCRP 156 transfer rate values should be investigated using other sets of data not employed in this investigation. For example, one might combine blood and bioassay data together for further validation and obtain better parameters that best fit the data. Care should be taken when using NHPs animal models. One must understand that the behavior of americium in human since is different than that of NHP as indicated by our results.

REFERENCES

Alomairy N, Brey RR, and Guilmette RA. ICRP 67 Biokinetic Models for Am-241 Applied to Nonhuman Primates. Health Physics 112: 423- 429; 2017.

Birchall A, Puncher M, Marsh JW, Bailey MR, Jarvis NS, Peach AD, Dorrian MD, and James AC. IMBA Professional Plus: A Flexible Approach to Internal Dosimetry. Radiation Protection Dosimetry; 2006.

Bureau Internation des Poids et Mesures, International Electrotechnical Commission, International Federation of Clinical Chemistry, International Organization for Standardization, International Union of Pure and Applied Chemistry, International Union of Pure and Applied Physics, International Organization of Legal Metrology. Evaluation of measurements data – guide to the expression of uncertainty in measurement. JCGM 100:2008; 2010.

Birchall A, Puncher M, Marsh JW, Davis K, Bailey MR, Jarvis NS, Peach AD, Dorrian M-D, James AC. IMBA Professional Plus: a flexible approach to internal dosimetry. Radiat Protect Dosim. 125:194–197; 2007.

Cam LL. Maximum likelihood: an introduction. Int Stat Rev 58(2):153-171; 1990.

Castellani CM, Marsh JW, Hurtgen C, Blanchardon E, Berard P, Giussani A, Lopez MA. IDEAS Guidelines (Version 2) for the Estimation of Committed Doses from Incorporation Monitoring Data. EURADOS Report 2013-01 [online]. EURADOS Report 2013-01. Available at http://eurados.org/~/media/Files/Eurados/documents/EURADOS%20Report%202013-01%20online%20version.pdf. Accessed 16 August 2015.

Doerfel H, Andrasi A, Bailey M, Berkovski V, Blanchardon E, Castellani CM, Hurtgen C, LeGuen B, Malatova I, Marsh J, Stather J. Guidelines for the estimation of committed doses from incorporation monitoring data. Project IDEAS-EU Contract No. FIKR-CT-2001-00160. 2006.

Doerfel H, Andrasi A, Bailey M, Berkovski V, Blanchardon E, Castellani CM, Hurtgen C, LeGuen B, Malatova I, Marsh J, Stather J. Internal dosimetry: the science and art of internal dose assessment. 2012. Available at: http://www.irpa.net/members/54302/%7B884C1520-D5CB-4908-94B4-954007C0F734%7D/RC%206%20Internal%20Dosimetry%20-%20The%20Science%20and%20Art%20of%20Internal%20Dose%20Assessment.pdf. Accessed January 1, 2017.

Durbin PW, Jeung N and Williams MH. Collected Original Data on Distribution of Americium-241 in Soft Tissues and Bones of Monkeys; 1990.

Durbin PW, Jeung N,Williams MH, Parrott MW, Kullgren B, Tuttle LW. Collected Original Data on Distribution of ^{241}Am in Bones of monkeys. Berkeley, CA: Division of Life Sciences, Lawrence Berkeley Laboratory; LBL-28649; 1993a.

Durbin PW, Jeung N,Williams MH, Parrott MW, Kullgren B, Tuttle LW. Collected Original Data on Distribution of ^{241}Am in Plasma, Whole Body, and Excreta of Monkeys. Berkeley, CA: Division of Life Sciences, Lawrence Berkeley Laboratory; LBL-28652; 1993b.

Etherington G, Stradling GN, Hodgson A., Fifield LK. Anomalously high excretion of Pu in urine following inhalation of plutonium nitrate. Radiat Prot Dosim 105(1-4): 321-324; 2003.

Gibbs RA, Rogers J, Katze MG, Bumgarner R, Winestock GM. Evolutionary and Biomedical Insights Fromthe Rhesus Macaque Genome. Science. 316:222–234; 2007.

Guilmette R.A, Cohen N, and Wrenn M.E. Distribution and Retention of 241Am in the Baboon. Radiation Research 81 (100-119); 1980.

Guilmette RA, Durbin PW, Toohey RE, Bertelli L. The NCRP Wound Model: Development and Application. Radiat Protect Dosim. 127:103–107; 2007.

Hurtgen C, Cossonnet C. A survey on uncertainties in bioassay measurements carried out with the ominex project. Radiat Prot Dosim: 105:375-378; 2003.

International Atomic Energy Agency (IAEA). Methods for assessing occupational radiation doses due to intakes of radionuclides. Safety Series No. 37. Vienna, 2004.

International Commission on Radiological Protection. Age dependent doses to members of public from intake of radionuclides: part 2, ingestion dose coefficients. Oxford: Pergamon Press; ICRP Publication 67; 1993.

International Commission on Radiological Protection. Individual Monitoring of Internal Exposure of Worker. ICRP publication 78; 1997.

Jacquez, J.A. Compartmental Analysis in Biology and Medicine. Amsterdam: Elsevier Publidhing Company, Amsterdam, 1972.

James AC. User manual for IMBA Professional Plus (Version 4.0). Richland, WA: AJC & Associates, Inc; 2005.

Kostecka K. Americium – From Discovery to the Smoke Detector and Beyond. Bull. His. Chem 33 (2); 2008.

Leggett R.W. A Retention-Excretion Model for Americium in Humans. Health Physics 62 (288-310); 1992.

Lloyd D.R, Mays C.W, Taylor G.N, and Atherton D.R. Americium-241 Studies in Beagles. Health Physics 18 (149-156); 1970.

Lloyd DR, Miller SC, Taylor GN, Bruenger FW, Angus W, Jee WSS. Comparison of Internal Emitter Radiobiology in Animals and Humans. Health Physics 72 (100-110); 1997.

Luciani RW. Plutonium Biokinetics in Human Body. PhD Dissertaion. Forschungszentrum Karlsruhe: Wissenschaftliche Berichte, FZKA 6748; 2002

McMurray, PJ. 1976 Hanford Americium Exposure Incident: Accident Description. Health Physics 45 (847-853); 1983.

National Council on Radiation Protection and Measurements. Development of a Biokinetic Model for Radionuclide-Contaminated Wounds and Procedures for Their Assessment, Dosimetry and Treatment. Bethesda, MD: NCRP; Report No. 156; 2007.

National Council on Radiation Protection and Measurements. Development of a Biokinetic Model for Radionuclide-Contaminated Wounds and Procedures for Their Assessment, Dosimetry and Treatment. Bethesda, MD: NCRP; Report No. 156; 2006.

Peterson J, MacDonell M, Haroun L, and Monette F. Radiological and Chemical Fact Sheets to Support Health Risk Analyses for Contaminated Areas. Argonne National Laboratory Environmental Science Division: 2007.

Puncher M, Birchall A, Marsh JW. The Autocorrelation Coefficient as a Tool for Assessing Goodness of Fit between Bioassay Predictions and Measurement Data. Radiat Protect Dosim.127:370–373; 2007.

Puncher A, and Birchall A. A Monte Carlo Method Calculation for Calculation Baysian Uncertainties in Internal Dodimetry. Radiation Protection Dosimetry; 2008.

Rosen J.C, Cohen N, and Wrenn M.E. Short Term Metabolism of ^{241}am in the Adult Baboon. Health Physics 22 (621-626); 1972.

Skrable KW, Chabot GE, French CS, LaBone TR. Intake retention functions and their applications to bioassay and the estimation of internal radiation doses. Health Phys 55(6):933-950;1988.

United States Nuclear Regulatory Commission (USNRC). Interpretation of bioassay measurements. NUREG/CR-4884; BNL-NUREG-52063. New York, NY; 1987. Available at: http://pbadupws.nrc.gov/docs/ML1128/ML11285A018.pdf. Accessed 1 January 2017.